COMPUTATIONAL FLUID DYNAMICS ANALYSIS OF A FREE/FORCED CONVECTION UNIT

HESAPLAMALI AKIŞKANLAR DİNAMİĞİ YÖNTEMİ İLE DOĞAL/ZORLAMALI KONVEKSİYON ÜNİTESİNİN İNCELENMESİ

IRMAK ASLANTÜRK

Submitted to
Hacettepe University
The Institute For Graduate Studies
in Science And Engineering
in partial fulfillmentof the requirements for the degree of
MASTER OF SCIENCE
in
NUCLEAR ENGINEERING

2010

To the Directory of the Institute for Graduate Studies in Science and Engineering,

This study has been accepted as a thesis for the degree of MASTER OF SCIENCE in NUCLEAR ENERGY ENGINEERING by our Examining Committee.

Head: :……
Assos. Prof. Dr. Murat Köksal

Advisor :…….
Prof. Dr. Üner Çolak

Member: :…….
Assos. Prof. Dr. Ayhan Yılmazer

Member: :…….
Assist. Prof. Dr. Şule Ergün

Member: :…….
Assist. Prof. Dr. Cemil Kocar

This is to certify that the Board of Directors of the Institute for Graduate Studies in Science and Engineering has approved this thesis on …/…/…..

Prof. Dr. Adil Denizli
Director
The Institute for Graduate Studies in Science and Engineering

COMPUTATIONAL FLUID DYNAMICS ANALYSIS OF A FREE/FORCED CONVECTION UNIT

Irmak Aslantürk

ABSTRACT

This thesis aims to model forced convection with air for simple and complicated heater geometries provided by abench topexperimental unit called Free/Forced Convection Unit which was designed and built by GUNT. It is used in laboratories of Department of Nuclear Engineering atHacettepe University. This stand has three heater surfaces and air at atmospheric pressure is used as coolant.

In this study, for the modeling and analysis, Computational Fluid Dynamics (CFD) technique is used. CFD is a numerical analysis method for fluid dynamics that uses finite volume method. With this method many different cases can be modeled such as heat, mass, momentum transfers or kinetic models.In this study CFD method is used to simulate experiments, simulation results and experimental data are compared.

Experiments are performed for three different heater elements. The first one is a flat plate in which there is no fin, and the second one is a finned type heater element in which parallel plates are mounted.The third one is pipe bundles in which fins are cylindrical tubes. These geometries are modeled in GAMBIT and analyses are performed by CFD method in FLUENT for three type heater elements. For each case four different turbulence models are used. These models are K-epsilon with standard wall functions near wall treatment, Spalart-Allmaras, K-omega, K-epsilon with enhanced wall treatment.

The most proper choice as the turbulence model for finned geometries is k-epsilon since the most accurate results with respect to analytical calculations are obtained when this model is used.

KEYWORDS: Forced Convection, air, heat transfer, Computational Fluid Dynamics

Advisor: Prof. Dr. ÜnerÇolak, Hacettepe University, Department of Nuclear Engineering, Nuclear Engineering Section

HESAPLAMALI AKIŞKANLAR DİNAMİĞİ YÖNTEMİ İLE DOĞAL/ZORLAMALI KONVEKSİYON ÜNİTESİNİN İNCELENMESİ

Irmak Aslantürk

ÖZ

Bu tezin amacı, basit ve karmaşık ısıtıcı geometrileri için hava ile zorlamalı konveksiyonun modellenmesdir. Bunun için, GUNT tarafından hazırlanan masa üstü Doğal/Zorlamalı Konveksiyon ünitesi kullanılmıştır. Bu ünite Hacettepe Nükleer Enerji Mühendisliği bölümü laboratuarlarında kullanılan bir aygıttır. Üç adet ısıtıcı yüzeyi vardır. Atmosfer basıncındaki hava soğutucu olarak kullanılır. Modelleme ve analizler için Hesaplamalı Akışkanlar Dinamiği(HAD) yöntemi kullanılmıştır. Bu metod ile ısı, kütle ve momentum transferi gibi birçok farklı durum için modellenebilmektedir. Bu çalışmada deneylerin simülasyonu için HAD yöntemi kullanılmış, çıkan sonuçlarla deneysel olarak elde edilen veriler incelenmiştir.

3 farklı ısıtıcı element için deneyler gerçekleştirilmiştir. Birincisi, dikey yüzeyleri olmayan düz plaka şeklindeki ısıtıcı, ikincisi plakaların paralel olarak yerleştirildiği dikey yüzeyli ısıtıcı element, üçüncüsü ise silindirik geometriye sahip dikey yüzeyleri olan ısıtıcı elementlerdir. Bu geometriler GAMBIT ile modellenmiş, FLUENT'te CFD yöntemi ile 3 farklı tip ısıtıcı element için analizler yapılmıştır. Her durum için dört farklı türbülans modeli kullanılmıştır. Bu modeller; "standard wall treatment "opsiyonuyla K-epsilon, Spalart-Allmaras, K-omega ve "enhanced wall treatment opsiyonuyla" K-epsilon'dur.

Deney verileri ve hesap sonuçlarının yapılabilmesi için hız, basınç farkı için deneysel gerekmektedir. Analitik sonuçlara en yakın değerler k-epsilon modeli kullanıldığında elde edildiği için, k-epsilon modeli, çalışmadaki deneylerin benzerlerinin yapılabilmesi için en uygun türbülans modelidir.

ANAHTAR SÖZCÜKLER: Zorlamalı Konveksiyon, air, ısı transferi, Hesaplamalı Akışkanlar Dinamiği

Danışman: Prof. Dr. Üner ÇOLAK, Hacettepe Üniversitesi, Nükleer Enerji Mühendisliği Bölümü, Nükleer Enerji Mühendisliği Anabilim Dalı

ACKNOWLEDGEMENTS

I am heartily thankful to my supervisor, Prof. Dr. ÜnerÇolak, whose encouragement, guidance and support enabled me to develop an understanding of the subject.

The quality of this study was greatly enhanced by the gracious assistance of Assist. Prof. Dr. ŞuleErgün.

Thanks also to Assoc. Prof. Dr. NiyaziSökmen, whose advice and help on FLUENT analysis was invaluable.

I would like to express my thanks to Res. Assist. Mehmet Türkmen for his help on every aspect of my thesis from the beginning to the end.

I offer my regards and blessings to my dear husband of his encouragments when I feel hopeless and his help during the completion of the study.

Lastly, I am grateful to my mother who has never stop standing behind me for my whole life.

TABLE OF CONTENTS

ABSTRACT i

ÖZ ii

ACKNOWLEDGEMENTS iii

LIST OF FIGURES vi

LIST OF TABLES viii

1 INTRODUCTION 1

1.1 Purpose and Content of Thesis 1

1.2 Computational Fluid Dynamics 2

1.3 FLUENT CFD Software 3

1.4 Heat Transfer 5

1.4.1 Convection Heat Transfer 6

1.5 Literature Review 11

2 PROBLEM STATEMENT 15

2.1 Definition 15

2.2 Free/Forced Convection Unit 15

2.2.1 Unit Set Up 15

2.2.2 Theoretical Principles 18

2.2.3 Experiments 19

3 COMPUTATIONAL FLUID DYNAMICS ANALYSIS 20

3.1 Pre-Processing (GAMBIT) 20

3.2 Solution Settings 22

3.2.1 Conservation Equation 22

3.2.2 Turbulence Models 25

3.2.3 Boundary Conditions 34

3.2.4 Other Properties 36

3.3 Post-Processing 38

3.3.1 Convergence 38
4 RESULTS ANDCONCLUSION 41
4.1 Results of CFD 41
4.1.1 Case 1 41
4.1.2 Case 2 44
4.1.3 Case 3 49
4.2 Results of Analytical Calculations 54
4.2.1 Case 1 54
4.2.2 Case 2 55
4.2.3 Case 3 57
4.3 Conclusion 59
5 RECOMMENDATIONS FOR FUTURE WORK 65
REFERENCES 66
APPENDIX 68
RESUME 69

LIST OF FIGURES

Figure 1.1 Schematic diagram of FLUENT analysis [10] 5
Figure 1.2 Example for Natural Convection 7
Figure 1.3 Example for Forced Convection 8
Figure 1.4 Tube arrangement in a bank for staggered design 9
Figure 2.1 Parts of Unit 15
Figure 2.2 Measurement points of Free/Forced Convection Unit for Pipe Bundles .. 17
Figure 2.3 Measurement points of Free/Forced Convection Unit for Parallel Fins.... 17
Figure 3.1 a) Flat type b) Finned type c) Pipe bundle 21
Figure 3.2 Mesh generation for pipe bundles 22
Figure 3.3 Boundary conditions of Free/Forced Convection Unit 36
Figure 3.4 Subdivisions of the near wall region 40
Figure 4.1 Velocity distribution with K-epsilon turbulence model using standard wall function (SWF) 42
Figure 4.2 Velocity distribution with k-epsilon turbulence model using enhanced wall treatment (EWT) 42
Figure 4.3 Velocity distribution with k-omega turbulence model 43
Figure 4.4 Velocity distribution with the Spalart-Allmaras turbulence model..... 43
Figure 4.5 Temperature distribution with k-epsilon turbulence model using standard wall function (SWF) 45
Figure 4.6 Velocity distribution with k-epsilon turbulence model using standard wall function (SWF) 45
Figure 4.7 Temperature distribution with k-epsilon turbulence model using enhanced wall treatment (EWT) 46
Figure 4.8 Velocity distribution with k-epsilon turbulence model using enhanced wall treatment (EWT) 46
Figure 4.9 Temperature distribution with k-omega turbulence model 47
Figure 4.10 Velocity distribution with k-omega turbulence model 47
Figure 4.11 Temperature distribution with the Spalart-Allmaras turbulence model... 48
Figure 4.12 Velocity distribution with the Spalart-Allmaras turbulence model..... 48
Figure 4.13 Temperature distribution with k-epsilon turbulence model using standard wall function (SWF) 49

Figure 4.14 Velocity distribution with k-epsilon turbulence model using standard wall function (SWF) 50
Figure 4.15 Temperature distribution with k-epsilon turbulence model using enhanced wall treatment (EWT) 50
Figure 4.16 Velocity distribution with k-epsilon turbulence model using enhanced wall treatment (EWT) 51
Figure 4.17 Temperature distribution with k-omega turbulence model 51
Figure 4.18 Velocity distribution with k-omega turbulence model 52
Figure 4.19 Temperature distribution with the Spalart-Allmaras turbulence model 52
Figure 4.20 Velocity distribution with the Spalart-Allmaras turbulence model 53
Figure 4.21 Comparison of different turbulent models and experimental result for cylindrical fins 63
Figure 4.22 Comparison of different turbulent models and experimental result for parallel fins 63
Figure 4.23 Comparison of different surface heat fluxes for cylindrical fins 63

LIST OF TABLES

Table 3.1 Cases and mesh properties 20
Table 3.2 Boundary conditions 36
Table 3.3 Turbulence model 1 37
Table 3.4 Turbulence model 2 37
Table 3.5 Turbulence model 3 37
Table 3.6 Turbulence model 4 37
Table 3.7 Boundary conditions for 3 Cases 38
Table 4.1Physical and geometrical data forCase 1 54
Table 4.2Physical and geometrical data for Case 2 55
Table 4.3Physical and geometrical data for Case 3 57
Table 4.4 Comparison of heat transfer and the Nusselt number for different turbulence models and analytical calculations for Case 1 60
Table 4.5 Comparison of heat transfer and the Nusselt number for different turbulence models and analytical calculations for Case 2 60
Table 4.6Comparison of heat transfer and the Nusselt number for different turbulence models and analytical calculations for Case 3 61
Table A-0.1 Constants of equation for the tube bank in cross flow 68
Table A-0.2 Correction factor C2 for NL< 20 ($Re_{D,max} \geq 10^3$) 68

1 INTRODUCTION

1.1 Purpose and Content of Thesis

The main purpose of this thesis is to model forced convection experiments performed in Free/Forced Convection unit by GUNT and to discuss the simulation capability of CFD calculation technique for these experiments.Moreover, various experiments can be simulated, so computer experiments can be performed with different parameters, results can be obtained by students for comparison, optimizations can be done easily with the help of the CFD software, and some new ideas about changing the design of the unit can be modeled.

The Free/Forced Convection Unit is modeled using three heaters which are listed below,

1. Flat plat
2. Finned plate
3. Pipe bundle

A total of 30 experiments are performed for all of these heater surfaces. In this study 6 experiments were performed (two for each surface) to learn how the unit works and find out how boundary conditions should be defined while modeling the unit. For the rest 24 experiments, data of the experiments performed by the students were used.Performing experiments was the first step of this study and will be explained later in detail.

The steps of studies which are performed are listed below,

1. Experiments are performed to gather the inputs.
2. CFD model is created by using the experimental results.
3. Analytical calculations.
4. Comparison of the results of CFD analysis and analytical calculations

After gathering the results of the experiments, approximate values for boundary conditions of each of the surfaces were found. These boundary conditions were the inputs of both the CFD models (2^{nd} step) and analytical calculations (3^{rd} step).

For the simulations, four different turbulence models were used at the second step of the study: k-epsilon, k-omega, and SpalartAllmaras. Each heater surface mentioned above was modeled using all of these turbulence models. FLUENT was the CFD software used for this purpose. Although there are some other options of CFD analysis software, FLUENT was selected since it is widely used and easily available.

At the third step, numerical analysis of each case is performed with four turbulent models expressed above with CFD. Velocity and temperature profiles are displayed for understanding the behavior of the flow.

Finally, to understand the results of FLUENT analysis and analytical calculations for each of the cases, comparisons are required. These comparisons displayed on graphs and figures. For each case heat transfer coefficients and Nusselt numbers are listed in tables. The reasons described for the best choice from the turbulence models.

1.2 Computational Fluid Dynamics

Computational Fluid Dynamics (CFD) is a numerical analysis method for fluid dynamics that uses finite volume or finite difference method. It has computationally-based design and analysis technique. It is possible to simulate all phases such as gases, liquids. Fluid flow is predicted by solving heat transfer, mass or flow transfer, and chemical reaction equations. In addition to that CFD method gives the opportunity to simulate extreme cases such as moving bodies, acousticsetc. CFD also has features for post-processing or in other words for simulating the performance of the data such as contours, pathlines and vectors [4], [9],[10].

The development of modern computational fluid dynamics began with the advent of the digital computer in the early 1950s. Finite difference methods (FDM) and finite element methods (FEM) are the basic tools used in CFD and have different origins. In 1910, at the Royal Society of London, Richardson presented a paper on the first FDM solution for stress analysis of a masonry dam. In contrast, the first FEM work was published in the Aeronautical science Journal by Turner, Clough, Martin and Topp for applications to aircraft stress analysis in 1955. Since then, both methods

have been developed extensively in fluid dynamics, heat transfer, and related areas [1].

CFD has widespread use of area and it supplies to imagine the physical phenomena related to the flow of any substance. It has many applications related with industry environment, medical, civil engineering, electronics etc.

CFD is widely used since faster and better analysis with shorter effort which saves time can be performed. Equipment improvements are built and installed with minimal downtime. CFD is a tool for compressing the design and development cycle. Also CFD can be chosen in the situation of when a prototype is hard to product; it enhances understanding of the designs. In addition by giving it different variables, optimal solution can be chosen from outputs in a shorter time.

The finite volume method is a discretization method. Various types such as elliptic, parabolic or hyperbolic of conservation laws may be simulated well using this method. It has some important features which are similar to those of the finite element method andboth of them may be used on arbitrary geometries. The finite volume method leads to robust schemes using structured or unstructured meshes. It has a feature that makes itself quite attractive when modeling problems such as fluid mechanics, semi-conductor device simulation, heat and mass transfer. The flux is of importance for all of these problems and the feature mentioned above is the local conservativeness of the numerical fluxes: the numerical flux is conserved from one discretization cell to its neighbor. Local conservativeness is provided by a balance approach: a local balance is written on each discretization cell which is often called “control volume”; by the divergence formula, an integral formulation of the fluxes over the boundary of the control volume is then obtained. The fluxes on the boundary are discretized with respect to the discrete unknowns [2]

1.3 FLUENT CFD Software

FLUENT is software for computational fluid dynamics (CFD). Its solvers are based on the finite volume method. In a widespread area, FLUENT is used as the help of their conceptual studies such as new designs, redesign,troubleshooting and optimization etc. This advanced technology results the analysis at a faster time and more accurate

way.It models turbulence, heat transfer and reactions for industrial applications such as combustion, air flow, or many other fluid types or wastewater treatment plant etc. By the additional properties, FLUENT has capability to model turbomachinary, multiphase systems [5].

FLUENT includes three main parts i.e. these are; pre-processor, solver, post-processor. In pre-processing part, geometry creation, mesh generation and mesh quality examination is being generated. After all, boundary zone assignment is defined to determine the solid, fluid parts and specifying boundaries of the computational domain. For these studies, FLUENT usesGAMBIT as a pre-processor; it supplies the input part of the analysis. In the solver part; initial conditions, boundary conditions are defined, material properties are determined. One of the physical models isselected. Operating conditions are prescribed. Also solution controls are set up. Finally conservation equations which are discretized are solved iteratively. FLUENT uses numerical solution technique.For this solution technique it uses finite volume method.

The steps of the numerical algorithm are formal integration of the governing equations over all the control volumes, discretization to convert integral equations into algebraic equations and the solution of these algebraic equations via iterative methods. The conservation of a flow variable Φwithin a control volume can be expressed as a balance as;

[Rate of change of ∅ in the control volume with respect to time] = [Net flux of ∅due to convection into the control volume] + [Net flux of ∅due to diffusion into the control volume] + [Net rate of creation of ∅inside the control volume]

the control volume integration of the conservation law for transport of a scalar having the general form is shown below;

$$\frac{\partial}{\partial t}\int_{V}\rho\phi dV+\oint_{A}\rho\phi\vec{U}\bullet dA=\oint_{A}\Gamma\nabla\phi\bullet dA+\int_{\forall}S_{\phi}dV \qquad (1.1)$$

The third and the last part of the analysis is post-processing part.For post-processing, different graphics are used such as vectors, pathlines, contours, and for all the grid

display. For each one temperature, pressure and so many properties can be examined to explicate the distribution of the variables. Eventually, this part supplies to visualize the results.

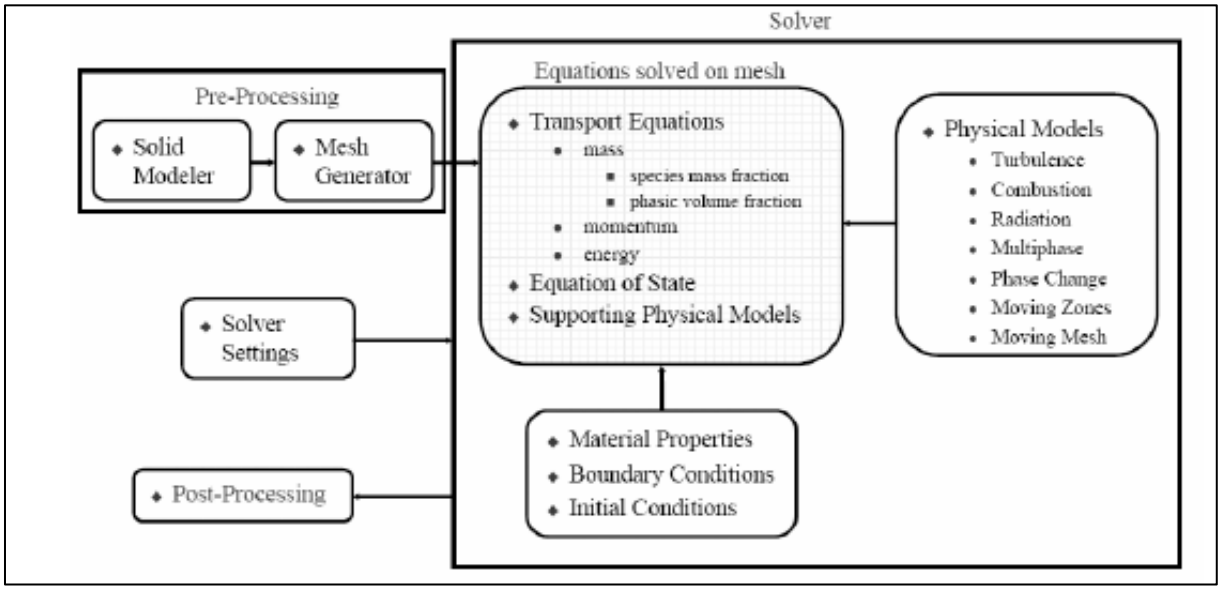

Figure 1.1 Schematic diagram ofFLUENT analysis [10]

1.4 Heat Transfer

Heat is the form of energy that can be transferred from one system to another as a result of temperature difference [11]. The amount of this transfer is the subject of thermodynamics analysis while heat transfer deals with the rate of the transfer (transfer per unit time).

Heat transfer is everywhere in our daily life. First of all human body is a source of heat itself and the comfort and even life of a person depends on heat. The refrigerators or ovens in the kitchen are two simple examples of so many practical application areas of heat transfer. So it is one of the important problems of many industrial and/or research areas such as automotive engineering, power plant engineering, materials processing, insulation, thermal systems, etc.

There are three heat transfer mechanisms: conduction, convection and radiation.

Conduction occurs at molecular level. When a temperature gradient exists in a medium (solid, liquid or gas), heat is transferred along that temperature gradient by

conduction [19]. More energetic particle of a substance transfers the energy to the adjacent less energetic ones as a result of interactions between the particles [11].

Convection is the transfer of heat by movement of fluids. It occurs between a fluid in motion and a bounding solid surface which are at different temperatures [6]. Heat transfer happens by random molecular motion (diffusion), and by bulk (or macroscopic) motion of the fluid. It can be said that occurs mostly by bulk fluid motion although molecular motion contributes to it. Because convective heat transfer is the subject of this thesis, it will be mentioned in some more detail later.

Radiation is the energy emitted by matter in the form of electromagnetic waves (or photons). It is the result of the changes in the electron configurations of the atoms or molecules [11]. While the conduction and convection requires the presence of an intervening medium, radiation does not. Energy transfer by radiation is the fastest mechanism of transfer (it happens at the speed of light) and it occurs most efficiently in a vacuum. Radiation is the mechanism of heat transfer from sun to the earth.

Detailed information about heat transfer can be found in [6], [11], [19].

1.4.1 Convection Heat Transfer

Depending on how the fluid movement is initiated, two types of convection exist: natural (or free) convection and forced (or assisted) convection.

Regardless of the particular nature of the convection heat transfer process, the rate equation is,

Newton's law of cooling[6],

$$q'' = h\,(T_s - T_\infty) \tag{1.2}$$

Where; q''= the convective heat flux (W/m^2)

h = convection heat transfer coefficient (W/m^{2}K)

T_s and T∞ is surface and fluid temperatures, respectively.

1.4.1.1 Modes of Convection

Modes of convection are examined in two parts. First one is natural convection and second one is forced convection. These convection types are briefly explained below.

Natural Convection

Natural convection is the transfer of heat by the circulation of fluids caused by natural means such as the buoyancy effect which can be shortly described as “the warmer fluid rises and the cooler fluid falls”. In other words, the fluid motion is driven by density differences associated with temperature changes generated by heating or cooling.

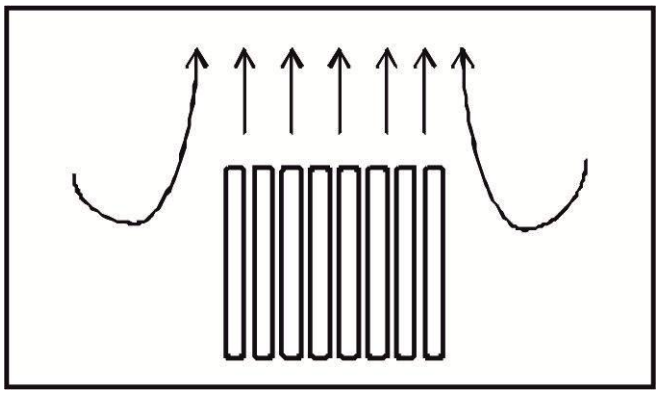

Figure 1.2 Example for Natural Convection

Forced Convection

Forced convection is the transfer of heat by the flow of fluids which are forced to flow by some external influences such as a pump or a fan. The fluid is forced to flow over a surface or in a pipe and convection is called as external convection or internal convection, respectively.

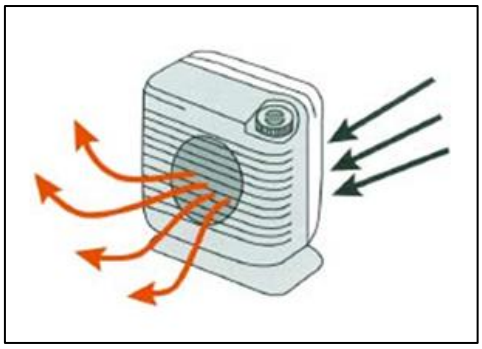

Figure 1.3 Example for Forced Convection

1.4.1.2 Geometry of Convection

Geometry of convection is examined in two parts. First one is external flow and second one is internal flow. Broadly, these flow types are described and required information for the calculations of the Nusselt number of both cases in the study is given below.

External Flow

To determine external flow, we can say that it is a flow in which boundary layers develop freely without any constraints.There is a region of the flow outside the boundary layer in which velocity and temperature gradients are negligible.

The system in which flat plate heater element is used behaves as external flow. And it is a special case such as there is an unheated part and from the point that unheated part finishes, heated part margin occurs.For the conditionswhich uses constant surface heat flux conditions for turbulent flow Nusselt number is calculated as;

$$Nu_x = 0.0308 Re_x^{4/5} Pr^{\frac{1}{3}} \quad (1.3)$$

If the heat flux is known, the convection coefficient can be used to determine the local surface temperature as below,

$$T_s(x) = T_\infty + \frac{q_s^{"}}{h_x} \tag{1.4}$$

$$(\overline{T_s - T_\infty}) = \frac{1}{L}\int_0^L (T_s - T_\infty)dx = \frac{q_s^{"}}{L}\int_0^L \frac{x}{Nu_x k}dx$$

$$(\overline{T_s - T_\infty}) = \frac{q_s^{"} L}{kNu_L}$$

So the nusselt number equation is,

$$\overline{Nu_L} = 0.05544 Re_L^{4/5} Pr^{\frac{1}{3}} \tag{1.5}$$

The other case in the study is flow across banks of tubes. There aremany applications of cross flow across tubes in industry such as steam generation in a boiler, air cooling of air condition, etc.

For calculations the arrangements for tubes are shown in Figure1.4 below,

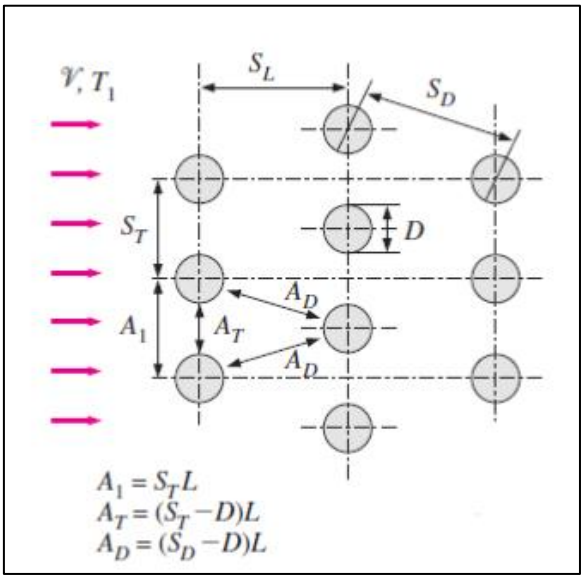

Figure 1.4 Tube arrangement in a bank for staggered design

Nusselt number is calculated as below in equation 1.7, [11]:

$$\overline{Nu_L} = C_2 C Re_{D,max}^{m} Pr^{0.36} \left(\frac{Pr}{Pr_s}\right)^{1/4} \tag{1.6}$$

m values can be read from Table A.1 in Appendix.

$$S_D = \left[S_L^2 + \left(\frac{S_T}{2}\right)^2\right]^{1/2} < \frac{S_t + D}{2} \tag{1.7}$$

Maximum velocity,

$$V_{max} = \frac{S_T}{2(S_T - D)} V \tag{1.8}$$

Reynolds number with respect to maximum velocity,

$$Re_{D,max} = \frac{V_{max} D}{\nu} \tag{1.9}$$

C constant is calculated as,

$$C = 0.35 * \left(\frac{S_T}{S_L}\right)^{1/5} \tag{1.10}$$

Fully developed region can be found,

$$\frac{I_e}{D} = 4.4\, Re^{1/6} \tag{1.11}$$

And friction factor is,

$$f = 0.316\, Re_D^{-\frac{1}{4}} \tag{1.12}$$

Internal Flow

A common application of heat transfer in both cooling and heating is flow through ducts or pipes. Motion of fluid is provided by a pump or fan to generate heat transfer. It is important to determine friction factor and convection coefficient because of their direct relation to pressure drop and convection coefficient. For determining pumping power requirement and the required tube length, the values defined above are used for calculations. It is important to determine difference between internal and external flow; as explained in external flow the fluid has a free surface in which boundary layer is free to grow but in internal flow; there occurs limitation by the inner surfaces.

For the case with finned heater element, there are short distances between fins thereforeit is assumed that the system is internal flow. Because of theoretical difficulties most correlations for the friction factor and heat transfer coefficients in turbulent flow are maintained experimentally. For sensitive results of the turbulent flow in tube banks, Petukhov equation is used for determining Nusselt number.

$$Nu_D = \frac{\left(\frac{f}{8}\right) Re_D Pr}{1.07 + 12.7\left(\frac{f}{8}\right)^{\frac{1}{2}}\left(Pr^{\frac{2}{3}} - 1\right)} \tag{1.13}$$

1.5 Literature Review

Computational Fluid Dynamics (CFD) is an important part of the research studies. In addition, although forced convection with finned geometries can be thought as a specific and hopefully narrower branch of CFD modeling studies, there are a large numberof studies in literature. However this study is based on an experimental set up and this is the point diverges from many other studies. In this part of the thesis, three similar studies are described along with common sides of a few studies about modeling forced convection with finned geometries using CFD method.

The aim of the study of A. Al-Sarkhi and E. Abu-Nada [15] is investigating the optimum number of fins and fin height for supplying best heat transfer over a finned tube in a vertial design which is subjected to forced convection. The equations were solved with control volume technique numerically. They focused on the idea of distributions of velocity and temperature depends on the height of the radial fins and number. They mentioned that maximum Nusselt number cannot be achieved at maximum height and fin number. The best configuration is shown on figures.

Another study which belongs to M. Tahat and et al [16]presents experimental study staggered and inline arrangements of the pin. The purpose is getting optimal spacings in specified directions. Also dependency of Nusselt number upon Reynolds number and pin fin pitch are accomplished.

N.Nagarani [18] investigates the heat transfer rate which depends on the fin's surface area he presented a study about heat transfer rate and efficiency of elliptical and circular annular fins. He realized that elliptical fin efficiency is better than circular one.

Another study [17] which is similar to ones summarized above is about the performance of heat transfer in circular fins in which T-section internal fins are inserted. The study of Md. Asharful Islam and A. K. Mozumder is carried out experimentally. For different Reynolds numbers for smooth and finned tubes, wall temperatures and pressure drop values measured. Corresponding to that, heat transfer coefficient, Nusselt number and friction factor of each case are calculated. At the end of the experiment it is observed that finned tube produces prominent heat transfer in contrast to smooth tubes.

In P.M. Guimarães and C.E.S. Da Silva's study [14] comparison between numerical and experimental results is performed for code validation. In their article, it is described that forced convection modeling is carried out in an enclosure. It has 18 stationary cylinders. Whole walls are assumed insulated except one which is allowed to transfer heat. In the upper side of the experimental set up there is a fan for movement of air. They presented temperature and velocity distributions to show their effect on the Nusselt number for the specified Reynolds number.

Another study that is similar to our study, using CFD method for modeling forced convection with finned geometries, is DenpongSoodphakdee, MuasudBehnia, and

David Watabe Copeland's study [12]. In this article, different fin geometries' performance is described. The aim is minimization of thermal resistance value at proper laminar air velocities and pressure gradients. Therefore different geometries are compared. Fin geometry examples are parallel plates or staggered plates and inline pin fins or staggered arrays. Computational Fluid Dynamics model bounded by planes of symmetry parallel to theflow are two dimensional and for reducing complexity they assumed three base points,

1. Heat transfer and fluid flow are two-dimensional.
2. Heat transfer and flow are periodically developed.
3. Thermal conductivity ratio of solid to fluid is quite high so the fins can be modeled as isothermal surfaces rather than conjugate solids

The air velocity approach is in the interval of 0.5 to 5 m/s. For these values, many analyses are performed for different geometries. They compared heat transfer performance and pressure drop, and showed that the highest heat transfer for a given combination of pressure gradient and flow rate was generally possible with the staggered plate fin geometry. In addition to that, the study is generated not only a single point but also for different values. It is presented that, staggered geometries show much performance than inline. But at low pressure drop values, elliptical fins suggest better performance in contrast to that, at higher values, round pins work best.

The study of Khan in [13] is subject to special consideration because of its similarities with our study in case of both the model and methodology.

One chapter of his doctorate thesis is related to numerical validation. In this chapter, he models the single circular pin and pin-fin heat sinks in a rectangular cabinet. These models are created by ICEPACK 3.2.12 which uses computational fluid dynamics method and finite volume method.

In the first part, inside the cabinetthere is a baseplate and a circular cylinder which is cooled by forced convection. The heat source is placed on the back side of the baseplate and three fans are used to force the air. This model is similar to my thesis. For the model, five numerical simulations are generated with different Reynolds numbers and the mass flow rate of the fans is calculated from the defined Reynolds

numbers based on the velocity. The results of ICEPACK are compared with the results of his analytical calculations in term of the average heat transfer coefficient. This is a point that our study is different from his: we used experimental data for our analytical calculations which are compared to the results of FLUENT; not the assumptions.

The properties are; steady and laminar flow, ignorance of natural flow and radiation, fluid is air and solid is extruded aluminum. After performing the model construction, the next step is mesh generation. Automatic mesh generation is a disadvantage of ICEPACK, because it is hard to construct finer mesh for complex geometries. After refinements, analysis is performed and he acquired the results such as velocity profile, temperature profile, xy plots... etc. Next step is to compare the analytically calculated heat transfer coefficients with the ones that are calculated by ICEPACK solutions for the specified Reynolds numbers and to find the error ratio for each of them.

In the second part, the model consists of a forced-convection-cooled pin-fin heat sink composed of a baseplate, a heat source at the center of the baseplate, and 49 pins uniformly spaced in in-line. The steps are the same as the previous one. And again the results are compared with the analytical values.

The small values of error ratios of both models in Khan’s study summarized above show that modeling with CFD method is convenient for cases of forced convection with geometries and this is an important and encouraging point for our study.

2 PROBLEM STATEMENT

2.1 Definition

Free/Forced Convection unitis a bench top unit which demonstrates and determines convectiveheat transfer experimentally. In the test stand, air is fed through a duct. During forced convection experiments, fan is going to be switched on and heating is carried out with three interchangeable heater elements.Data information can be read by electronic sensors such as the temperature and air velocities are measured using sensors. The measured values can be read on digital displays and the measured data can be transferred from the display and control unit to a PC by USB.

2.2 Free/Forced Convection Unit

2.2.1 Unit Set Up

Parts of the unit and functionalities of the unit are described below.

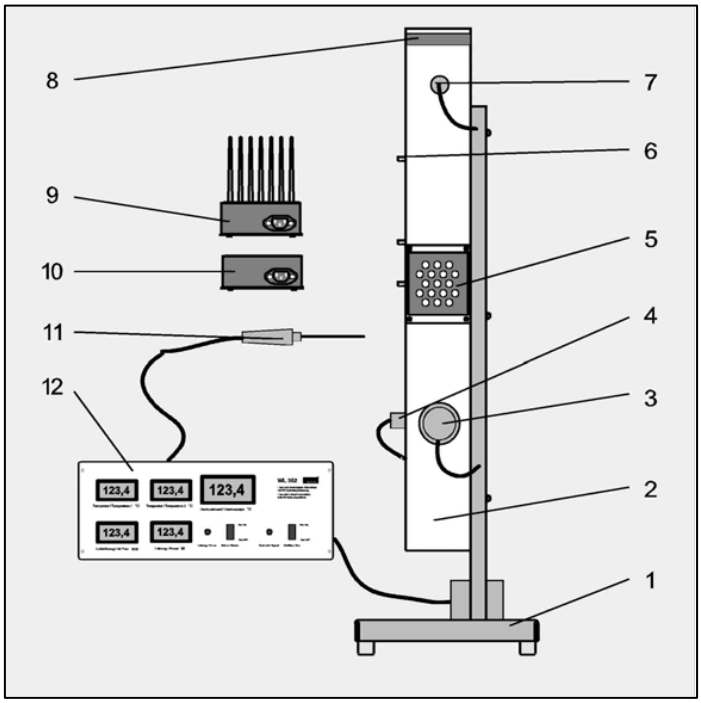

Figure 2.1 Parts of Unit

1. Experimental unit with holder
2. Air duct: It is a guide to flow the air. Cross section of 120 x 120 mm2 and a length of 1m.
3. Flow sensor: It records the flow rate of the inlet air and two temperature sensors.
4. Temperature sensor: It records inlet temperature.
5. Heater element “pipe bundle”: It is mounted using simple toggle type fasteners in the duct. Pipe bundle is one of the hated surfaces which is heated with a maximum total output of approximately 170W.
6. Measuring glands for thermocouple.
7. Temperature sensor: It records outlet temperature.
8. A built-in fan: It supplies to transmit the flow by different applied speed values.
9. Heater element “finned”: It is mounted using simple toggle type fasteners in the duct. Pipe bundle is one of the heater surfaces which is heated with a maximum total output of approximately 170W.
10. Heater element“flat plate”: It is mounted using simple toggle type fasteners in the duct. Pipe bundle is one of the hated surfaces which is heated with a maximum total output of approximately 170W.
11. Thermocouple type K: It enables to record temperature at various points.
12. Display and control unit:
    It contains;
    i. power supply
    ii. regulators for the fan and heater inserts.

Also this unit displays,

i. the electrical power supplied to the heater elements,
ii. the flow rate,
iii. the inlet and outlet air temperature
iv. the temperature measured with the thermocouple.[3]

Measurement points of the Unit are displayed in Figure 2.2 for cylindrical fins and in Figure 2.3 for parallel fins.

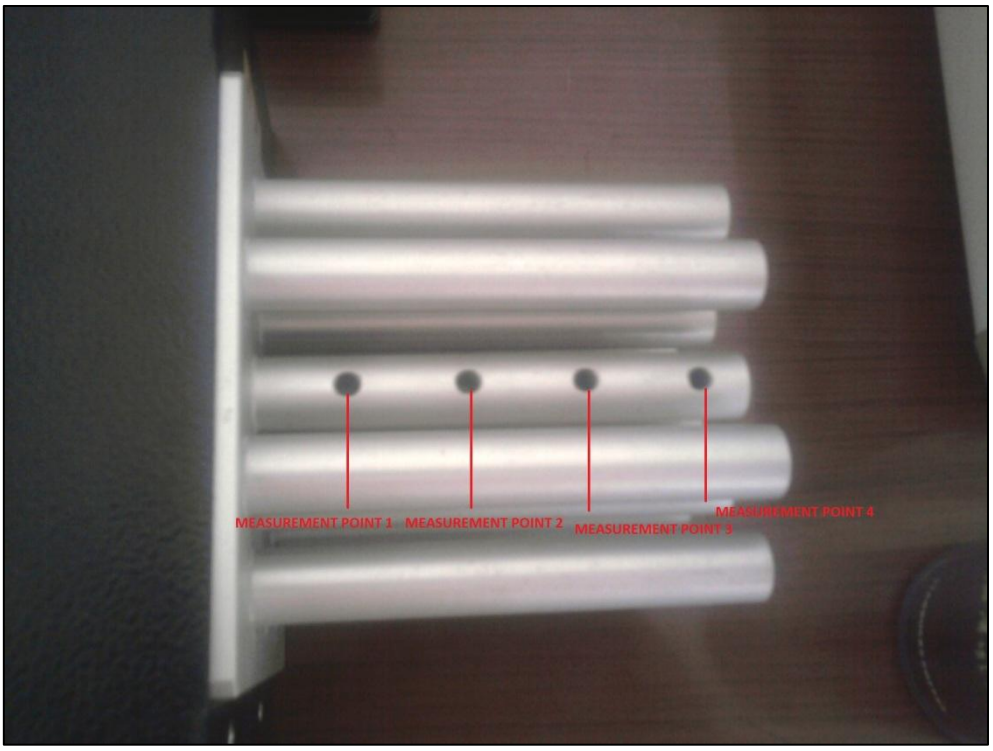

Figure 2.2 Measurement points of Free/Forced Convection Unit for Pipe Bundles

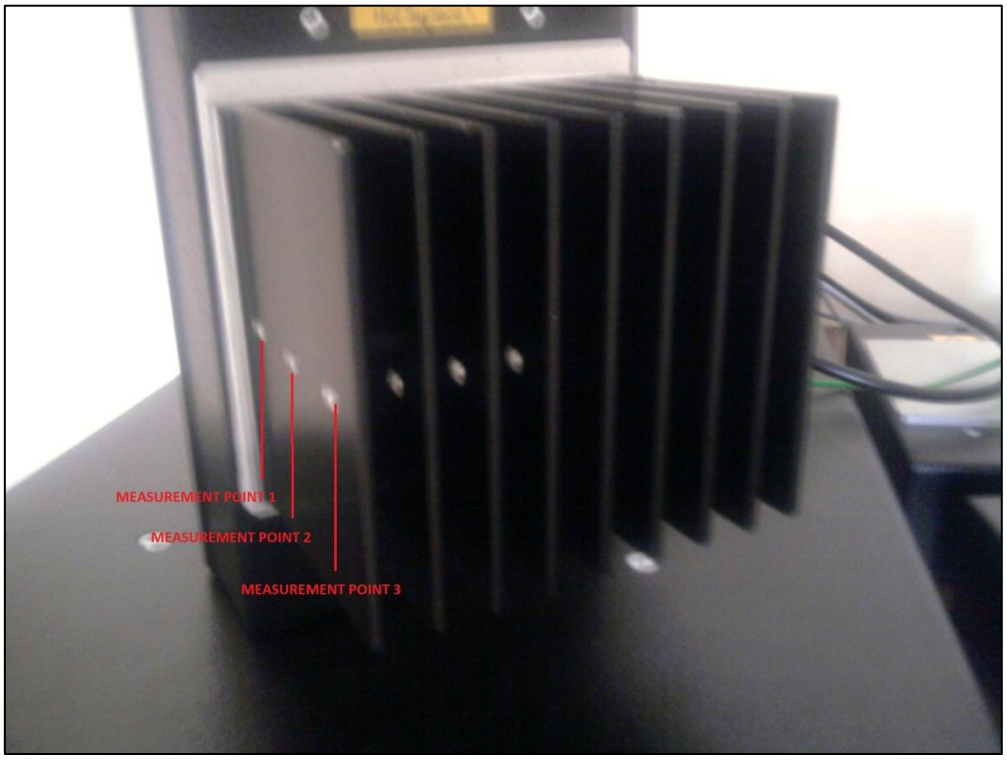

Figure 2.3 Measurement points of Free/Forced Convection Unit for Parallel Fins

2.2.2 Theoretical Principles

Theoretical formulas are described as below

$$Q = \dot{m}\ Cp\ \Delta T \tag{2.1}$$

WhereQ is amount of heat

$$\dot{m}\ = w\ A\ \rho_{air} \tag{2.2}$$

where $\dot{m}$ is air mass flow,w is flow rate over the entire cross-sectional area of the flow.

The cross-sectional area A is set at a constant 0.0144 m^2 on the Test Stand for Free and Forced Convection.

Reynolds number is a criterion for defining whether flow is turbulent or laminar.

$$Re = \frac{w\ l}{\gamma}, for\ flat\ plates \tag{2.3}$$

$$Re = \frac{wd}{\gamma}, forcylinders \tag{2.4}$$

Nusselt number is dimensionless measure of heat transfer. It ispractice to nondimensionalize the heat transfer coefficient h with the Nusselt number which is defined as,

$$Nu = \frac{hL_c}{k} \tag{2.5}$$

Where k is thermal conductivity of the fluid, L_c is the characteristic length.Nusselt number represents the enhancementof heat transfer through a fluid layer as a result of convection relativeto conduction across the same fluid layer. The larger the Nusselt number,the more effective the convection. A Nusselt number of Nu =1 for a fluidlayer represents heat transfer across the layer by pure conduction.

2.2.3 Experiments

Experiments are carried out in such a way;

Heater element with a flat plate is connected to the unit. For data acquisition, control unit connected to a computer. Potentiometer on the control unit is set to 100 % and surface temperature is measured after reaching steady state condition. The values are recorded; air flow rate at the inlet, inlet temperature and outlet temperature. By using Equation (2.1) the amount of heat that is transferred is calculated.

By using the datawhich are recorded by the students in laboratories, optimal values are chosen for inlet temperature and heat flux to use in FLUENT analysis.

3 COMPUTATIONAL FLUID DYNAMICS ANALYSIS

In this chapter for CFD analysis, the schematic diagram displayed in Figure 1.1 is carried out.The first part of this chapter is pre-processing of modeling. Construction is achieved by GAMBIT (Geometry and Mesh Building Intelligent Toolkit) which is an integrated program for CFD analysis.The second part is solution settings in which conservation equations, turbulence models, boundary conditions and other related parameters are expressed for FLUENT analysis.Finally in the third section, the convergence circumstancesare determined and post-processes of the analysis are displayed.

3.1 Pre-Processing (GAMBIT)

The first part of the FLUENT analysis is the construction of the model. Computational subdomains (grids) are generated in GAMBIT which is the preprocessor of FLUENT. The system consists of a duct and three interchangeable heater elements mounted to the unit. For each heater element, a model is constructed. The solid and fluid regions were set according to the unit design. It is 70 cm high and 12 x 12 cm base area.

20 cm above the bottom of the unit, the interchangeable heater elements are mounted.

In case 1, flat plate is mounted. In case 2,finned type heater element is mounted. There are 9 plates each are 0.4-cm-thick and 7.1-cm-long which are perpendicular to the flow also each are 10-cm-long along flow and in case 3, pipe bundle type heater element is analyzed. There are 17 bundles which are 9.7-cm-long perpendicular to the flow.Mesh type and average total elements are described for each case in the table below. Computational subdomains are shown in Figure 3.1

Table 3.1 Cases and mesh properties

Heater element type	Mesh type	Total elements
Flat plate	Hexagonal map	336.000
Finned	Hexagonal supmap	1.200.000
Pipe bundle	Hexagonal map*	1.180.000

*For pipe bundles hex-cooper mesh type is used and boundary layers applied.

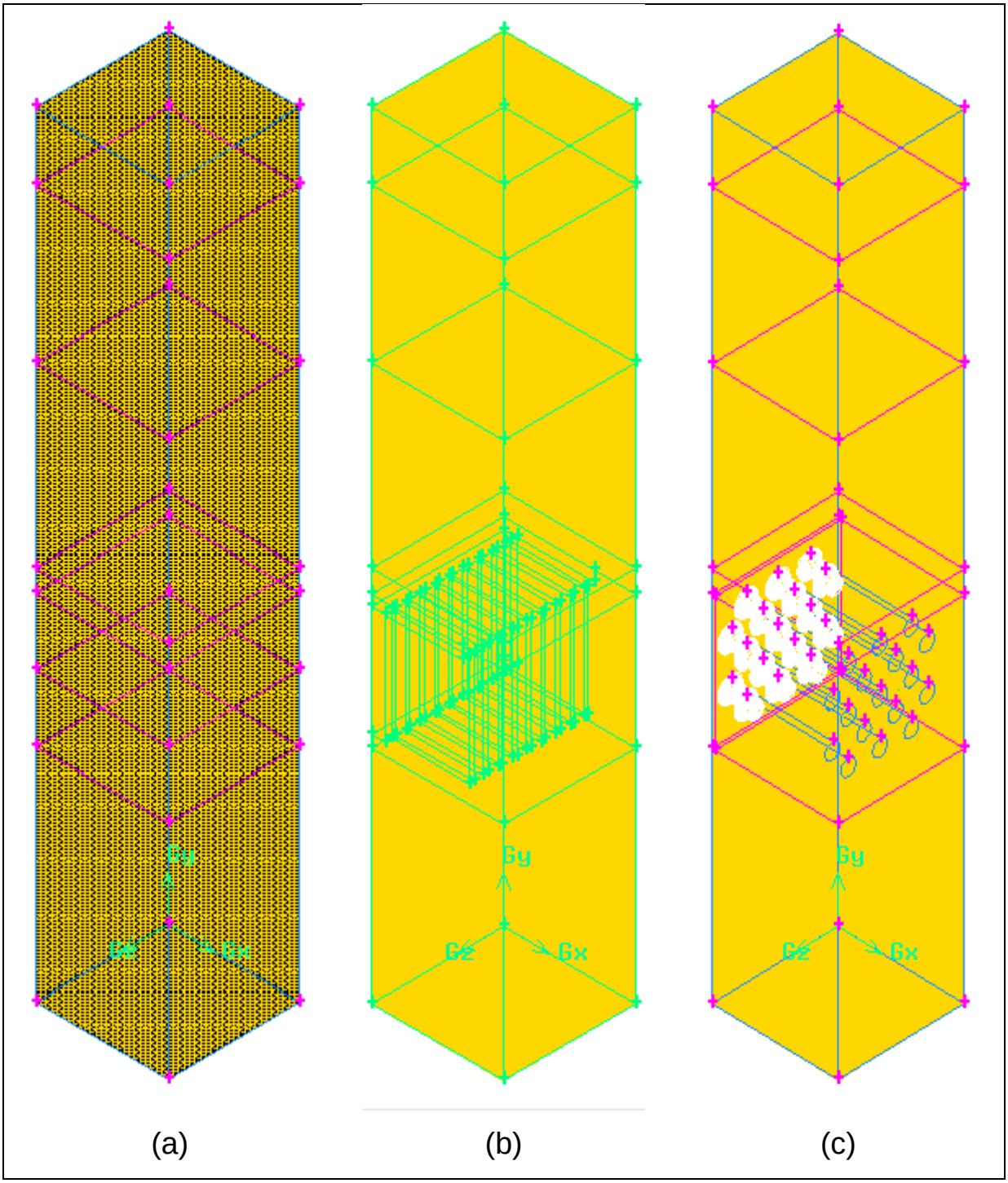

Figure 3.1 a) Flat type b) Finned type c) Pipe bundle

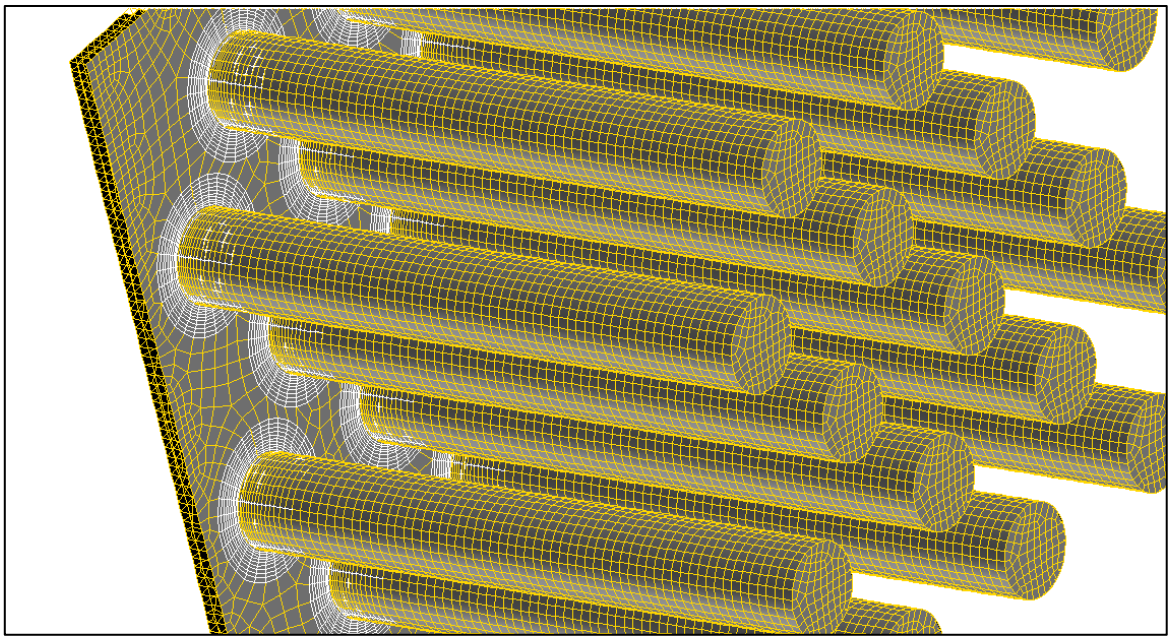

Figure 3.2 Mesh generation for pipe bundles

3.2 Solution Settings

After preparing the case in GAMBIT such as finishing the preparation of grids, specifying boundary and continuum types, other specifications are defined in FLUENT such as material properties, boundary conditions, initial conditions, operating conditionsetc.

Before that, it is given below how FLUENT solves numerically, which equations are used.

3.2.1 Conservation Equation

Conservation equations for mass and momentum are solved for all flows in FLUENT. However in this study, heat transfer modeling is used therefore an additional equation for energy conservation is solved.[7]

3.2.1.1 Mass Equation

The equation for conservation of mass, or continuity equation, can be written as follows:

$$\frac{\partial \rho}{\partial t} + \nabla.(\rho \vec{v}) = S_m \quad (3.1)$$

This equation is the general form of the mass conservation equation and is valid for incompressible as well as compressible flows. The source S_m is the mass added to the continuous phase from the dispersed second phase (e.g., due to vaporization of liquid droplets) and any user-defined sources. But in this study there occurs no second phase or user defined functions, then the equation becomes;

$$\frac{\partial \rho}{\partial t} + \nabla.(\rho \vec{v}) = 0 \quad (3.2)$$

3.2.1.2 Momentum Equation

Conservation of momentum equation is given below;

$$\frac{\partial (\rho \vec{v})}{\partial t} + \nabla.(\rho \vec{v} \vec{v}) = -\nabla p + \nabla.(\bar{\bar{\tau}}) + \rho \vec{g} + \vec{F} \quad (3.3)$$

where p is the static pressure, $\bar{\bar{\tau}}$ is the stress tensor, $\rho\vec{g}$ is gravitational body force and the last term in the right hand side, $\vec{F}$ is external body force.

The stress tensor $\bar{\bar{\tau}}$is given by;

$$\bar{\bar{\tau}} = \mu[(\nabla \vec{v} + \nabla \vec{v}^T) - \frac{2}{3}\nabla.\vec{v}I](3.4) \quad (3.4)$$

where$\mu$is the molecular viscosity, I is the unit tensor, and the second term on the right hand side is the effect of volume dilation. [8]

3.2.1.3 Energy Equation

Since heat transfer model is preferred, energy equation will be solved. The equation is written below;

$$\frac{\partial(\rho E)}{\partial t} + \nabla.(\vec{v}(\rho E + p)) = -\nabla.(k_{eff}\nabla T - \sum_j h_j \vec{J}_j + (\overline{\overline{\tau}}.\vec{v}) + S_h \quad (3.5)$$

where$k_{eff}$is the effective conductivity (k + k_t, wherek_t is the turbulent thermal conductivity,

$\vec{J}_j$is the diffusion flux of species j.

The first three terms on the right-hand side of equation represent energy transfer due to conduction, species diffusion, and viscous dissipation, respectively.

$S_h$includes the heat of chemical reaction, and any other volumetric heat sources that is defined.

In Equation (3.5)

$$E = h - \frac{p}{\rho} + \frac{v^2}{2} \quad (3.6)$$

where sensible enthalpy h is defined for ideal gases as;

$$h = \sum_j Y_j h_j \quad (3.7)$$

and for incompressible flows as;

$$h = \sum_j Y_j h_j + \frac{p}{\rho} \quad (3.8)$$

In Equations (3.7) and (3.8),Y_j is the mass fraction of species j and;

$$h_j = \int_{T_{ref}}^{T} c_{p,j} dT \quad (3.9)$$

where$T_{ref}$is 298.15 K.

For solid regions energy equation is shown below;

$$\frac{\partial(\rho h)}{\partial t} + \nabla.(\vec{v}\rho h) = -\nabla.(\mathrm{k}\nabla T) + S_h \quad (3.10)$$

whereρ is density,

h is sensible enthalpy,

k is conductivity, t is temperature

S_h is volumetric heat source.

The second term on the left-hand side of Equation 3.10 represents convective energy transfer due to rotational or translational motion of the solids. The velocity field $\vec{v}$is computed from the motion specified for the solid zone. The terms on the right-hand side of Equation 3.10are the heat flux due to conduction and volumetric heat sources within the solid, respectively.

3.2.2 Turbulence Models

Turbulence is a fluid regime which is unsteady, irregular in space and time, 3 dimensional. In addition to these features, it is strongly diffusive. It is a continuum phenomenon. Turbulence is a term stands to understand the behavior of motions of fluid since it shows complex and unpredictable behavior. Turbulent flow is random and rapid fluctuations of eddies. Fluctuations reveal supplement methods for the calculations of momentum and heat transfer [21].In that case, aturbulence model consists of equations for the requirement of determination of unknown turbulent correlations that comes from the process.Turbulence models are simulated with the Navier-Stokes (NS) and continuity equations.[11], [20].

As determined before in the study FLUENT is used for CFD applications. And FLUENT presents the options for turbulence models signified below;

- Spalart-Allmaras
- K-epsilon (k-ϵ) model
- K-omega (k –ω) model
- Reynolds stress model (RSM)
- Large Eddy Simulation

In this chapter all these models are discussed but mainly focused on Spalart-Allmaras, K-epsilon (k- ϵ) model, K-omega (k –ω) model since for CFD analysis, these models are preffered. Detailed information is given in [7].

3.2.2.1 Spalart-Allmaras model:

The Spalart-Allmaras model is a one-equation model that is designed specifically for aerospace applications. This model is started to be used in turbomachinery applications. It solves the transport equation for the kinematic eddy (turbulent) viscosity.

This model type is preferred for relatively crude simulations on coarse meshes where accurate turbulent flow computations are not critical. But originally this model is a low-Reynolds-number model. Furthermore, the near-wall gradients of the transported variable in the model are much smaller than the gradients of the transported variables in the k-epsilon or k-omega models. This might make the model less sensitive to numerical error when non-layered meshes are used near walls. One-equation models are often criticized for their inability to rapidly accommodate changes in length scale, such as might be necessary when the flow changes abruptly from a wall-bounded to a free shear flow. The Spalart and Allmaras model which employs the Boussinesq approach solves transport equation in a form of turbulent kinematic viscosity.

The transported variable in the Spalart-Allmaras model, $\check{\nu}$, is identical to the turbulent kinematic viscosity except in the near-wall (viscous-affected) region. The transport equation for $\check{\nu}$is

$$\frac{\partial}{\partial x}(\rho\check{\nu}) + \frac{\partial}{\partial x_i}(\rho\check{\nu}u_i) = G_\nu + \frac{1}{\sigma_{\check{\nu}}}\left[\frac{\partial}{\partial x_j}\left\{(\mu + \rho\check{\nu})\frac{\partial\check{\nu}}{\partial x_j}\right\} + C_{b2}\rho\left(\frac{\partial\check{\nu}}{\partial x_j}\right)^2\right] - Y_\nu + S_{\check{\nu}} \qquad (3.11)$$

whereG_ν is the production of turbulent viscosity.

$Y_\nu$is the destruction of turbulent viscosity that occurs in the near-wall region due to wall blocking and viscous damping.

$\sigma_{\tilde{\nu}}$and$C_{b2}$are constants and $\nu$is the molecular kinematic viscosity.

$S_{\tilde{\nu}}$is a user-defined source term.

Since the turbulence kinetic energy k is not calculated in the Spalart-Allmaras model, the last term in Equation 3.11 is ignored when estimating the Reynolds stresses.

The turbulent viscosity,μ_t, is computed from

$$\mu_t = \rho\tilde{\nu}f_{\tilde{\nu}1} \tag{3.12}$$

where$f_{\tilde{\nu}1}$is the viscous damping function.

3.2.2.2 K-epsilon (k- ϵ) model:

K-ϵ is two-equation and semi-empirical model. It gives almost accurate for a wide range of turbulent flows. In subparts more detailed definitions will be defined. This model divides into three parts; RNG, standard and realizable. They both have similarities but differences in the method of calculating turbulent viscosity, the turbulent Prandtl numbers governing the turbulent diffusion of k and ϵ, the generation and destruction terms in the ϵ equation and the generation and destruction terms ϵ in the equation.The features that are essentially common to all models follow, including turbulent production, generation due to buoyancy, accounting for the effects of compressibility, and modeling heat and mass transfer.

<u>Standard k-epsilon (k- ϵ) model:</u>

It is a semi-empirical model based on model transport equations for the turbulence kinetic energy k and its dissipation rate, and the derivation of the model equations relies on phenomenological considerations and empiricism. The simples "complete models" of turbulence are two-equation models in which the solution of two separate transport equations allows the turbulent velocity and length scales to be independently determined. This type is popular in industrial flow and heat transfer simulations. In a consequence of strengths and weaknesses of the standard k-ϵmodel, improvements have been made to improve its performance. The model transport equation k is derived from the exact equation, while the model transport

equation for ϵ was obtained using physical reasoning and bears little resemblance to its mathematically exact counterpart.

It is important that, in the derivation of the k-ϵ model, the assumption is that the flow is fully turbulent, and the effects of molecular viscosity are negligible. The standard k-ϵ model is therefore valid only for fully turbulent flows.

The turbulence kinetic energy, k, and its rate of dissipation, ϵ, are obtained from the following transport equations:

$$\frac{\partial}{\partial x}(\rho k) + \frac{\partial}{\partial x_i}(\rho k u_i) = \frac{\partial}{\partial x_j}\left[(\mu + \frac{\mu_t}{\sigma_k})\frac{\partial k}{\partial x_j}\right] + G_k + G_b - \rho\epsilon - Y_M + S_k \quad (3.13)$$

and

$$\frac{\partial}{\partial t}(\rho\epsilon) + \frac{\partial}{\partial x_i}(\rho\epsilon u_i) = \frac{\partial}{\partial x_j}\left[(\mu + \frac{\mu_t}{\sigma_\epsilon})\frac{\partial \epsilon}{\partial x_j}\right] + C_{1\epsilon}\frac{\epsilon}{k}(G_k + C_3 G_b) - C_{2\epsilon}G_b\rho\frac{\epsilon^2}{k} + S_\epsilon \quad (3.14)$$

where$G_k$represents the generation of turbulence kinetic energy due to the mean velocity gradients.

G_b represents the generation of turbulence kinetic energy due to buoyancy.

YM represents the contribution of the fluctuating dilatation in compressible turbulence to the overall dissipation rate.

$C_{1\epsilon}$, $C_{2\epsilon}$ and $C_{3\epsilon}$are constants.

$\sigma_k$and$\sigma_\epsilon$are the turbulent Prandtl numbers for k and ϵ, respectively.

$S_k$and$S_\epsilon$are user-defined source terms.

The turbulent (or eddy) viscosity ,μ_t, is computed by combining k and ϵ as follows:

$$\mu_t = \rho C_\mu \frac{k^2}{\epsilon} \tag{3.15}$$

where$C_\mu$is a constant.

RNG k-epsilon (k- ϵ) model:

The RNG k-ϵmodel was derived using renormalization group theory. Despite the form of the RNG k-ϵmodel is similar to the standard k-ϵmodel, this model includes refinements. One of them is for accuracy improvement for rapidly strained flow; this model has an additional term in its ϵ equation. The other one is the effect of swirl on turbulence is included in the RNG model, enhancing accuracy for swirling flows. The third one is standard k-ϵmode uses user-specified, constant values although the RNG theory provides an analytical formula for turbulent Prandtl numbers. And one more refinement is while the standard k-ϵmodel is a high-Reynolds-number model, the RNG theory provides an analytically-derived differential formula for effective viscosity that accounts for low-Reynolds-number effects. But the feature is related to appropriate treatment of the near-wall region.

All these properties, refinements make the model more accurate and reliable for a wider class of flows than the standard k-ϵmodel.

The RNG k-ϵmodel has a similar form to the standard k-ϵ model:

$$\frac{\partial}{\partial x}(\rho k) + \frac{\partial}{\partial x_i}(\rho k u_i) = \frac{\partial}{\partial x_j}(\mu_{eff}\alpha_k \frac{\partial k}{\partial x_j}) + G_k + G_b - \rho\epsilon - Y_M + S_k \tag{3.16}$$

and

$$\frac{\partial}{\partial t}(\rho\epsilon) + \frac{\partial}{\partial x_i}(\rho\epsilon u_i) = \frac{\partial}{\partial x_j}(\mu_{eff}\alpha_\epsilon \frac{\partial \epsilon}{\partial x_j}) + C_{1\epsilon}\frac{\epsilon}{k}(G_k + C_{\epsilon 3}G_b) - C_{2\epsilon}G_b\rho\frac{\epsilon^2}{k} - R_\epsilon + S_\epsilon \tag{3.17}$$

In these equations, $G_k$represents the generation of turbulence kinetic energy due to the mean velocity gradients

$G_b$is the generation of turbulence kinetic energy due to buoyancy,

$Y_M$represents the contribution of the fluctuating dilatation in compressible turbulence to the overall dissipation rate.

The quantities $\alpha_k$and $\alpha_\epsilon$are the inverse effective Prandtl numbers for k and ϵ, respectively.

$S_k$and$S_\epsilon$are user-defined source terms.

The scale elimination procedure in RNG theory results in a differential equation for turbulent viscosity:

$$d\left(\frac{\rho^2 k}{\sqrt{\epsilon\mu}}\right) = 1.72\frac{\check{\nu}}{\sqrt{\check{\nu}^3 - 1 + C_\nu}}d\check{\nu} \tag{3.18}$$

Equation 3.18 is integrated to obtain an accurate description of how the effective turbulent transport varies with the effective Reynolds number (or eddy scale), allowing the model to better handle low-Reynolds-number and near-wall flows. In the high-Reynolds-number limit, Equation 3.18 gives

$$\mu_t = \rho C_\mu \frac{k^2}{\epsilon} \tag{3.19}$$

Where C_μ is constant.

Realizable k-epsilon (k-ϵ) model

The realizable k-ϵmodel differs from the standard k-ϵmodel in two important ways: The realizable k-ϵmodel contains a new formulation for the turbulent viscosity. And a new transport equation for the dissipation rate, ϵ, has been derived from an exact equation for the transport of the mean-square vorticity fluctuation.

The term "realizable" means that the model satisfies certain mathematical constraints on the Reynolds stresses, consistent with the physics of turbulent flows constraints. Neither the standard k-ϵmodel nor the RNG k-ϵmodel is realizable.

Realizable k-ϵmodel differs from the other k-ϵmodels in accuracy of the spreading rate of both planar and round jets. In addition to that it supplies performance for flows involving rotation, boundary layers under strong adverse pressure gradients, separation, and recirculation.

The modeled transport equations for k and ϵ in the realizable k-ϵmodel are

$$\frac{\partial}{\partial t}(\rho k) + \frac{\partial}{\partial x_i}(\rho k u_i) = \frac{\partial}{\partial x_j}\left[(\mu + \frac{\mu_t}{\sigma_k})\frac{\partial k}{\partial x_j}\right] + G_k + G_b - \rho\epsilon - Y_M + S_k \quad (3.20)$$

and

$$\frac{\partial}{\partial x}(\rho\epsilon) + \frac{\partial}{\partial x_i}(\rho\epsilon u_i) = \frac{\partial}{\partial x_j}\left[(\mu + \frac{\mu_t}{\sigma_\epsilon})\frac{\partial \epsilon}{\partial x_j}\right] + \rho C_1 S_\epsilon + C_{1\epsilon}\frac{\epsilon}{k}C_{3\epsilon}G_b - C_2\rho\frac{\epsilon^2}{k + \sqrt{\nu\epsilon}} + S_\epsilon \quad (3.21)$$

As in other k-ϵmodels, the eddy viscosity is computed from

$$\mu_t = \rho C_\mu \frac{k^2}{\epsilon} \quad (3.22)$$

The difference between the realizable k-ϵmodel and the standard and RNG k-ϵmodels is that $C_\mu$is no longer constant.

3.2.2.3 K-omega (k –ω) model:

Shear-Stress Transport (SST) k-ω model

The shear-stress transport (SST) k-ω model was developed to effectively blend the robust and accurate formulation of the k-ω model in the near-wall region with the free-stream independence of the k-ω model in the far field. To achieve this, the k –ϵmodel is converted into a k-ω formulation. The SST k-ω model is similar to the standard k-ω model, but includes the following refinements: The modeling constants

are different. The standard k-ω model and the transformed k-ϵ model are both multiplied by a blending function and both models are added together. The blending function is designed to be one in the near-wall region, which activates the standard k-ω model, and zero away from the surface, which activates the transformed k-ω model.

The SST k-ω model has a similar form to the standard k-ω model:

$$\frac{\partial}{\partial t}(\rho k) + \frac{\partial}{\partial x_i}(\rho k u_i) = \frac{\partial}{\partial x_j}\left[\Gamma_k \frac{\partial k}{\partial x_j}\right] + \widetilde{G_k} - Y_k + c \qquad (3.23)$$

$$\frac{\partial}{\partial t}(\rho \omega) + \frac{\partial}{\partial x_i}(\rho \omega u_i) = \frac{\partial}{\partial x_j}\left[\Gamma_\omega \frac{\partial \omega}{\partial x_j}\right] + G_\omega - Y_\omega + S_\omega + D_\omega \qquad (3.24$$

In these equations, $\widetilde{G_k}$represents the generation of turbulence kinetic energy due to mean velocity gradients,

$G_\omega$represents the generation of ω,

$\Gamma_k$and$\Gamma_\omega$represent the effective diffusivity of k and ω, respectively,

$Y_k$and$Y_\omega$represent the dissipation of k and ωdue to turbulence,

$D_\omega$represents the cross-diffusion term,

$S_\omega$and$S_\omega$are user-defined source terms.

The turbulent viscosity, μ_t, is computed as follows:

$$\mu_t = \frac{\mathrm{k}\rho}{\omega} \frac{1}{max\left[\frac{1}{\alpha}, \frac{SF_2}{\omega a_1}\right]} \qquad (3.25)$$

Standard k-ω model

The standard k-ω model is an empirical model based on model transport equations for the turbulence kinetic energy k and the specific dissipation rate ω. The standard k-ω model incorporates modifications for low-Reynolds-number effects, compressibility, and shear flow spreading. The model predicts free shear flow spreading rates that are in close agreement with measurements for far wakes, mixing

layers, and plane, round, and radial jets, and is thus applicable to free shear flows and wall-bounded flows. And by the modifications for accurate results for free shear flows, production terms have been added.

The turbulence kinetic energy, k, and the specific dissipation rate, ω are obtained from the following transport equations:

$$\frac{\partial}{\partial t}(\rho k) + \frac{\partial}{\partial x_i}(\rho k u_i) = \frac{\partial}{\partial x_j}\left[\Gamma_k \frac{\partial k}{\partial x_j}\right] + G_k - Y_k + S_k \qquad (3.26)$$

$$\frac{\partial}{\partial t}(\rho \omega) + \frac{\partial}{\partial x_i}(\rho \omega u_i) = \frac{\partial}{\partial x_j}\left[\Gamma_\omega \frac{\partial \omega}{\partial x_j}\right] + G_\omega - Y_\omega + S_\omega \qquad (3.2$$

In these equations, $G_k$represents the generation of turbulence kinetic energy due to mean velocity gradients. $G_\omega$represents the generation of ω. $\Gamma_k$and $\Gamma_\omega$represent the effective diffusivity of k and ω, respectively. $Y_k$and$Y_\omega$represent the dissipation of k and ω due to turbulence. All of the above terms are calculated as described below. $S_k$and$S_\omega$are user-defined source terms.

The turbulent viscosity,$\mu_t$is computed by combining k and ω as follows:

$$\mu_t = \alpha \frac{k\rho}{\omega} \qquad (3.28)$$

3.2.2.4 Reynolds stress model (RSM)

The Reynolds stress model (RSM) is more detailed model than others. RSM closes the Reynolds-averaged Navier-Stokes equations by solving transport equations for the Reynolds stresses, together with an equation for the dissipation rate. Five additional transport equations are required in 2D flows and seven additional transport equations must be solved in 3D.

Since the RSM accounts for the effects of streamline curvature, swirl, rotation, and rapid changes in strain rate, it has greater potential to give accurate predictions for complex flows. However, the fidelity of RSM predictions is still limited by the closure assumptions employed to model various terms in the exact transport equations for the Reynolds stresses.

RSM model should be preferred when we are dealing with cyclone flows, highly swirling flows in combustors, rotating flow passages, and the stress-induced secondary flows in ducts.

3.2.2.5 Large Eddy Simulation

Turbulent flows are characterized by eddies with a wide range of length and time scales. The largest eddies are typically comparable in size to the characteristic length of the mean flow. The smallest scales are responsible for the dissipation of turbulence kinetic energy.

By the approach of the direct numerical simulation (DNS), it is possible that whole spectrum of turbulent scales can be resolved but practically it is not suitable for high Reynolds number flows because of the increase of the cost.

In large eddy simulation, large eddies are resolved directly, while small eddies are modeled. The justification for the selection of LES is; momentum, mass, energy, and other passive scalars are transported mostly by large eddies. Large eddies are more problem-dependent. They are dictated by the geometries and boundary conditions of the flow involved but conversely small eddies are less dependent on the geometry, tend to be more isotropic, and are consequently more universal.

If large eddies are chosen, much coarser meshes and larger times-step sizes will be in LES than in DNS but LES still requires substantially finer meshes than those typically used for RANS calculations. In addition, LES has to be run for a sufficiently long flow-time to obtain stable statistics of the flow being modeled. As a result, the computational cost involved with LES is normally orders of magnitudes higher than that for steady RANS calculations in terms of memory (RAM) and CPU time. Therefore, high-performance computing (e.g., parallel computing) is a necessity for LES, especially for industrial application [7].

3.2.3 Boundary Conditions

In this part of the thesis boundary conditions are defined. Continuum and boundary types are specified in GAMBIT. FLUENT has the feature to change the boundary

condition that is defined in GAMBIT. This property supplies not to be back to GAMBIT.

For the determination of the conditions for inlet and outlet, there occur many properties such as pressure inlet, pressure outlet, velocity inlet, mass flow inlet…etc. In this case there is a fan. This provides forced convection. Velocity inlet at inlet and pressure outlet at outlet is defined as boundary condition. Other boundary types remain as wall boundary condition. For defining the heating element after selecting wall boundary condition, heat flux value is entered which is calculated from the experimental values. Finally for continuum zones solid and fluid options are selected and for solid zone, aluminum is selected as material type for fluid zone, air is selected as a material type.

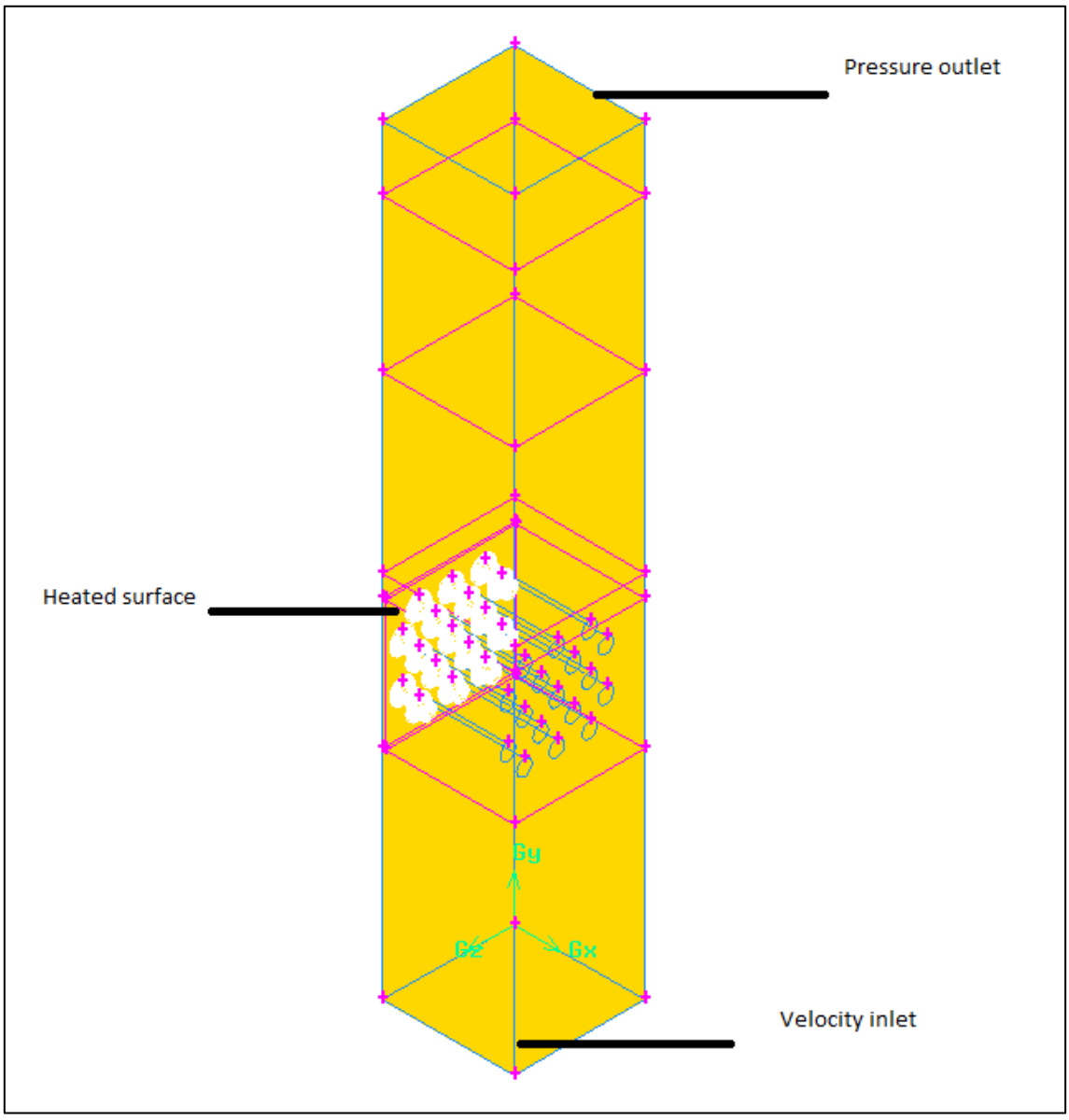

Figure 3.3 Boundary conditions of Free/Forced Convection Unit

3.2.4 Other Properties

In this step, firstly material properties are defined. For solid regions, aluminum material type is selected. For fluid regions air type material is selected.

Then operating conditions are determined. Since heat transferis solved in the problem, gravity term should be activated. It is in –y direction, -9.8 /s2. And also operating density is also activated for the same reason.

Finally, in Table 3.2 the conditions are same for all heater elements.For each of the cases; viscous type in Table 3.3, Table 3.4, Table 3.5 and Table 3.6 is used in analysis.

Table 3.2 Boundary conditions

Boundary	Boundary condition type
Inlet	Velocity inlet
Outlet	Pressure outlet
Solver Panel Options	
Solver	Pressure Based
Space	3D
Formulation	Implicit
Velocity Formulation	Absolute
Gradient Option	Green-Gauss Cell Based
Time	Steady
Operating Conditions Panel Options	
Pressure	Operating Pressure (Pa)=101325 Reference Pressure Location X(m)=0 Y(m)=0 Z(m)=0
Gravity	Gravity Acceleration X(m/s^2)=0 Y(m/s^2)=- 9.81

	Z(m/s^2)=0
Variable-Density Parameters	Operating Density (kg/m3)=1.225

Table 3.3 Turbulence model 1

Viscous Panel Option (Step 1)	
Model	k-epsilon
k-epsilon model	Realizable
Near-wall treatment	Standard Wall Functions
Model Constants	Default

Table 3.4 Turbulence model 2

Viscous Panel Option (Step 2)	
Model	k-epsilon
k-epsilon model	Realizable
Near-wall treatment	Enhanced wall treatment
Model Constants	Default

Table 3.5 Turbulence model 3

Viscous Panel Option (Step 3)	
Model	Spalart-Allmaras
Spalart-Allmaras Options	Vorticity-Based Production
Model constants	Default

Table 3.6 Turbulence model 4

Viscous Panel Option (Step 4)	
Model	k-omega

k-omega model	Standard
k-omega options	Shear flow corrections
Model constants	Default

For the model, the boundary conditions are in Table3.7 below;

Table 3.7 Boundary conditions for 3 Cases

	Flat plate	Finned	Pipe Bundle
Inlet velocity (m/s)	2.76	2.66	2.18
Inlet Temperature (K)	295.35	295.40	295.42
Heat Flux (w/m^{2}K)	3520.48	7198.24	6689.32
Turbulent Intensity(%)	10	10	10
Hydraulic Diameter(m)	0.12	0.12	0.12
Flow Direction	Upward	Upward	Upward

3.3 Post-Processing

3.3.1 Convergence

In CFD modeling in order to understand whether a simulation is leading to reliable results or not, convergence must be checked. This check can be done by performing the following:

- Checking - overall massbalance
  - overall momentum balance
  - energy balance
- Observing convergence parameters – checking residuals to see whether the values of the residuals of two consecutive iterations are similar or not. In addition, variation in residuals should agree with what is expected for a steady state simulation.

In the analyses, pressure based option is selected as the solver type. Therefore, the energy residual is expected to decrease to a value of 10^{-6}.

In order to increase the sensitivity of the analysis, discretizationis changed to second order upwind from first order upwind throughout the calculations.

If the above mentioned methods do not provide the convergence, mesh refinement is performed.

For Cases 1 and 2, no convergence problem was observed since in these cases the geometry is simple.To model Case 3, i.e., the unit with pipe bundle heater element, mesh refinement is required. For mesh refinement, boundary layer is defined in detail around the pipe bundles.

Since acontinuous domain is defined discretely, the degree to which the salient features of the flow such as boundary layersare resolved depends on the density and distribution of nodes in the mesh.

As stated in FLUENT manual: “Resolution of the boundary layer such as mesh spacing near wallsalso plays a significant role in the accuracy of the computed wall shear stress and heat transfer coefficient. This is particularly true in laminar flows where the grid adjacent to the wall should obey,

$$y_p\sqrt{\frac{u_\infty}{vx}} \leq 1 \qquad (3.29)$$

wherey_p= distance to the wall from the adjacent cell centroid

u_∞= free-stream velocity

v= kinematic viscosity of the fluid

x= distance along the wall from the starting point of the boundary layer”

For turbulent flows proper resolution of the mesh is also very important. In this study, the flow is turbulent. Due to the strong interaction of the mean flow and turbulence, the numerical results for turbulent flows tend to be more susceptible to grid dependency than those for laminar flows. In the near-wall region, different mesh resolutions are performed as defined above. It is defined in Fluent manual that, “The

near-wall region can be subdivided into three layers. In the innermost layer, called the "viscous sublayer", the flow is almost laminar, and the (molecular) viscosity plays a dominant role in momentum and heat or mass transfer. In the outer layer, called the fully-turbulent layer, turbulence plays a major role. Finally, there is an interim region between the viscous sublayer and the fully turbulent layer where the effects of molecular viscosity and turbulence are equally important. Figure 3.4 illustrates these subdivisions of the near-wall region, plotted in semi-log coordinates."

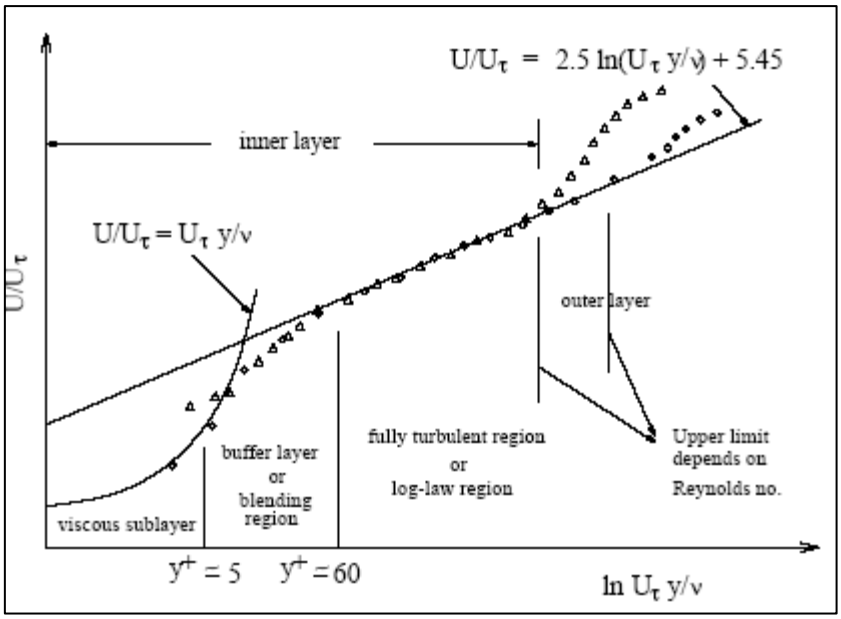

Figure 3.4 Subdivisions of the near wall region

In Figure 3.4,

$$y^+ \equiv \frac{\rho u_t y}{\mu} \tag{3.30}$$

where$u_t$is the friction velocity, defined as $\sqrt{\frac{\tau_w}{\rho}}$. [7]

With respect to these y^+values, refinements are performed. As the result of all calculations performed for all cases, convergence is achieved.

4 RESULTS ANDCONCLUSION

In this chapter, analytical calculations are performed and the results of CFD analysis are compared with these results.

4.1 Results of CFD

4.1.1 Case 1

In case 1, flat plate heater element is used in experimental setup and in the modeling.

The velocity profiles in axial (y) direction are presented in Figures 4-1, 4-2, 4-3 and 4-4. The velocity profile shown in these figures are for a plane placed at the middle of the unit in x-direction.

As figures indicate different turbulence models show different velocity profiles since for each turbulent equation code uses different solution strategy.

By examining the profiles, it is observed that; by the influence of the heater element which is a flat plate, velocity starts to increase in axial direction. It is the effect of heat transfer arises from the heater element. In this case, no-slip option was selected in shear condition part so near wall boundaries in which at the interface between the fluid and the surface, attraction occurs between molecules of the solid and fluid. This force reduces bulk velocity. As a result of this, bulk velocity is zero at the wall and increases as the fluid is far away from the wall. So the profile modeled is as expected.

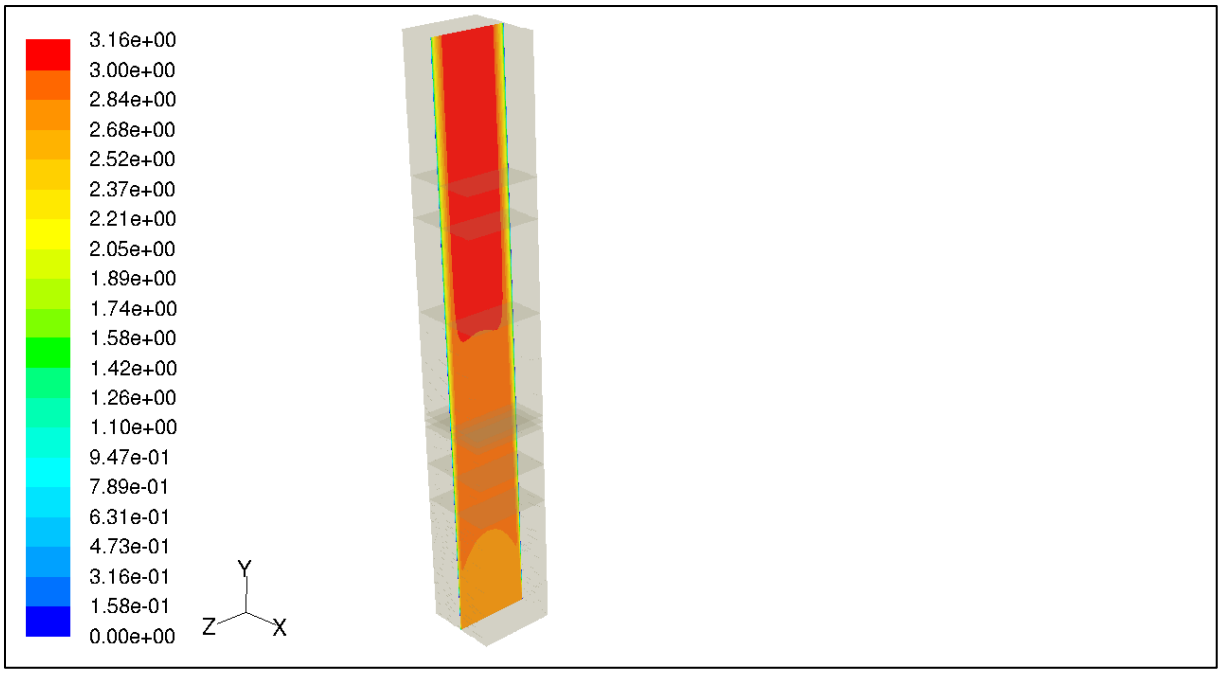

Figure 4.1 Velocity distribution with K-epsilon turbulence model using standard wall function (SWF)

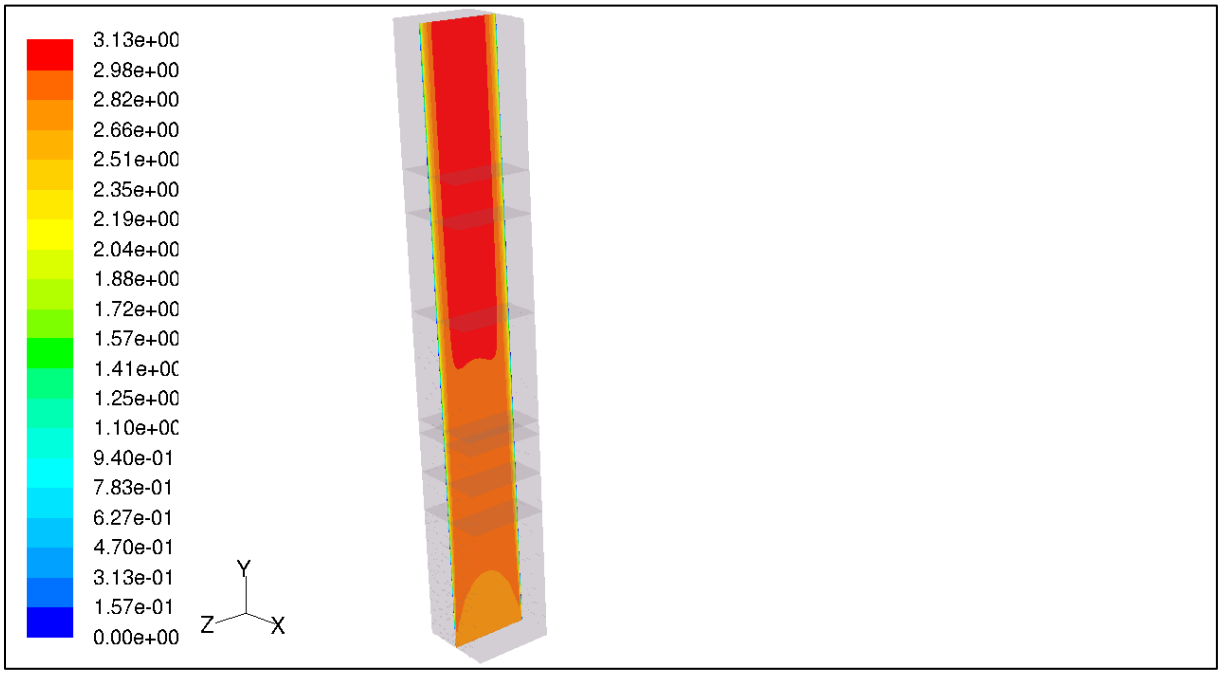

Figure 4.2 Velocity distribution with k-epsilon turbulence model using enhanced wall treatment (EWT)

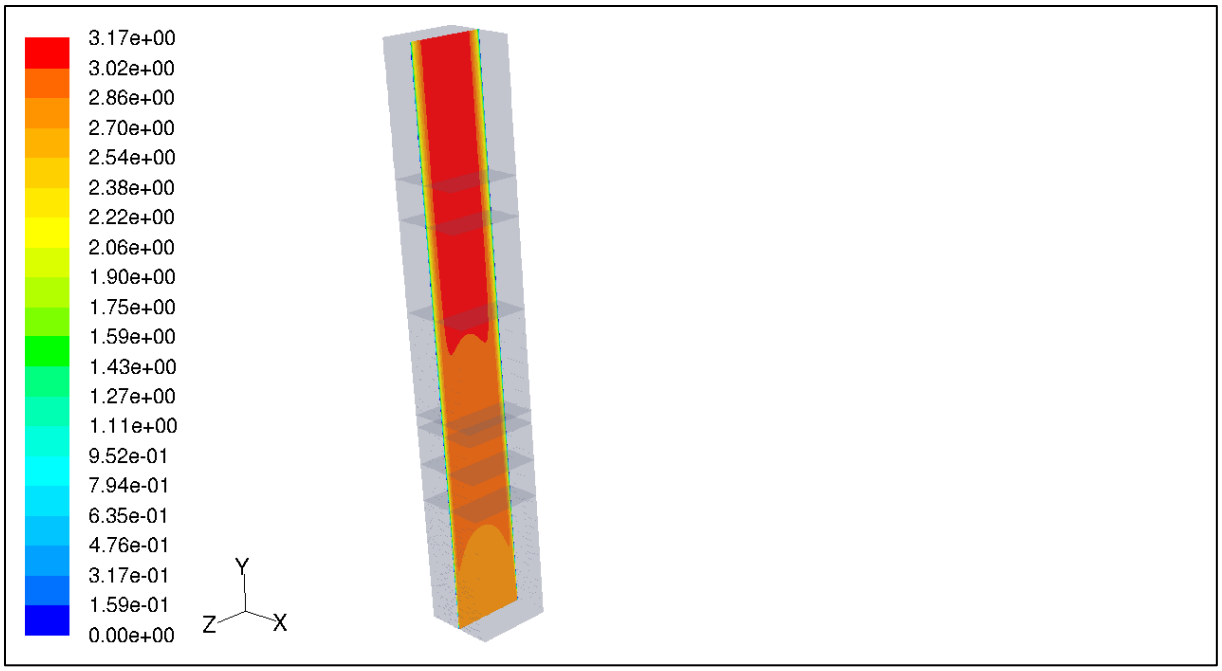

Figure 4.3 Velocity distribution with k-omega turbulence model

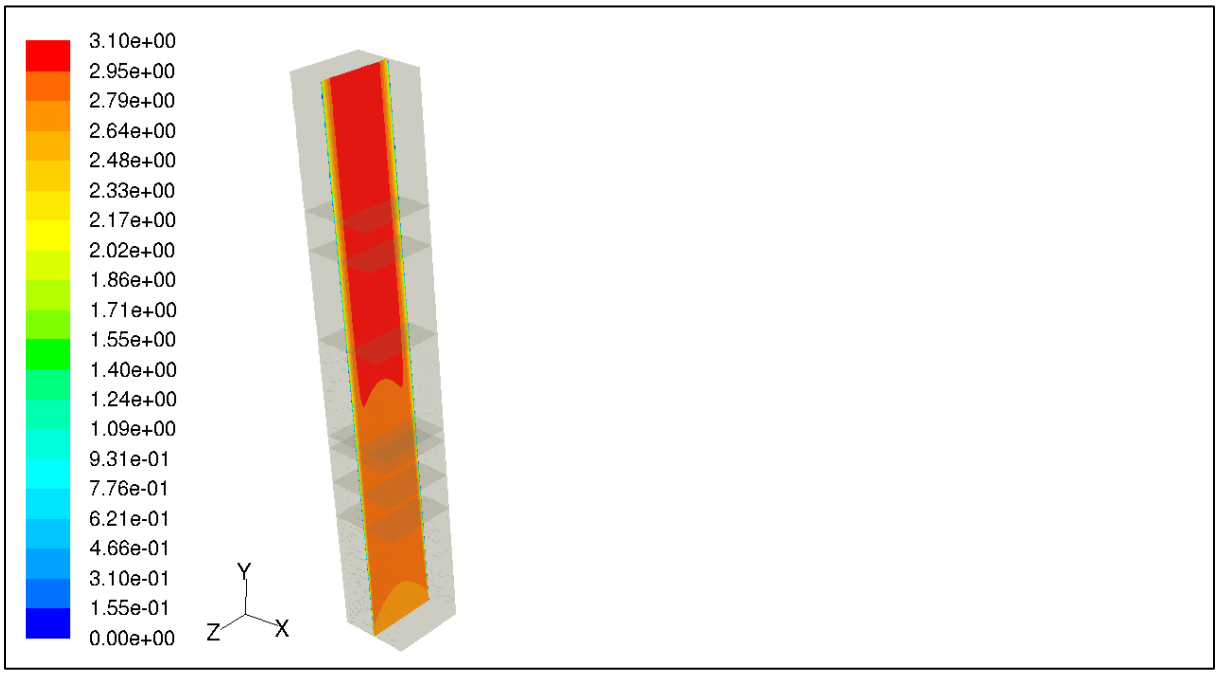

Figure 4.4 Velocity distribution with the Spalart-Allmaras turbulence model

4.1.2 Case 2

In case 2, finned heater element is used in experimental setup and in the modeling. In this part, temperature and velocity profiles are displayed. Here the sectioning is perpendicular to the flow and in the middle of the fins. Temperature profiles for the specified turbulence models are displayed in Figures 4-5, 4-7, 4-9, 4-11. Velocity profiles are displayed in Figures 4-6, 4-8, 4-10, 4-12.During Fluent analysis, for the heater elements, both conduction through the fins and convection are solved as 'coupled'.

Boundary condition for the heater element surface was defined as constant surface heat flux, as can be observed from the cross-section of the temperature profile, as far away from that surface, temperature decreases. By the impact of the forced air with a fan at the top, temperature values decreases along the fin length. In other words, heat transfer occurs. In the base part of the fins, heat transfer is better than at the end of the fin since temperature difference is higher. Velocity reaches maximum values in between the fins as far away from the walls and also in between the end of the fins and the outer domain. Fins provide better heat transfer since they increase heat transfer area. As the velocity increases Reynolds number gets higher and turbulence occurs or increases. As a result of this better heat transfer conditions can be achieved since turbulence enhances the heat transfer. In addition velocity increases as the flow passes through the fins since the total flow area is restricted with fins.

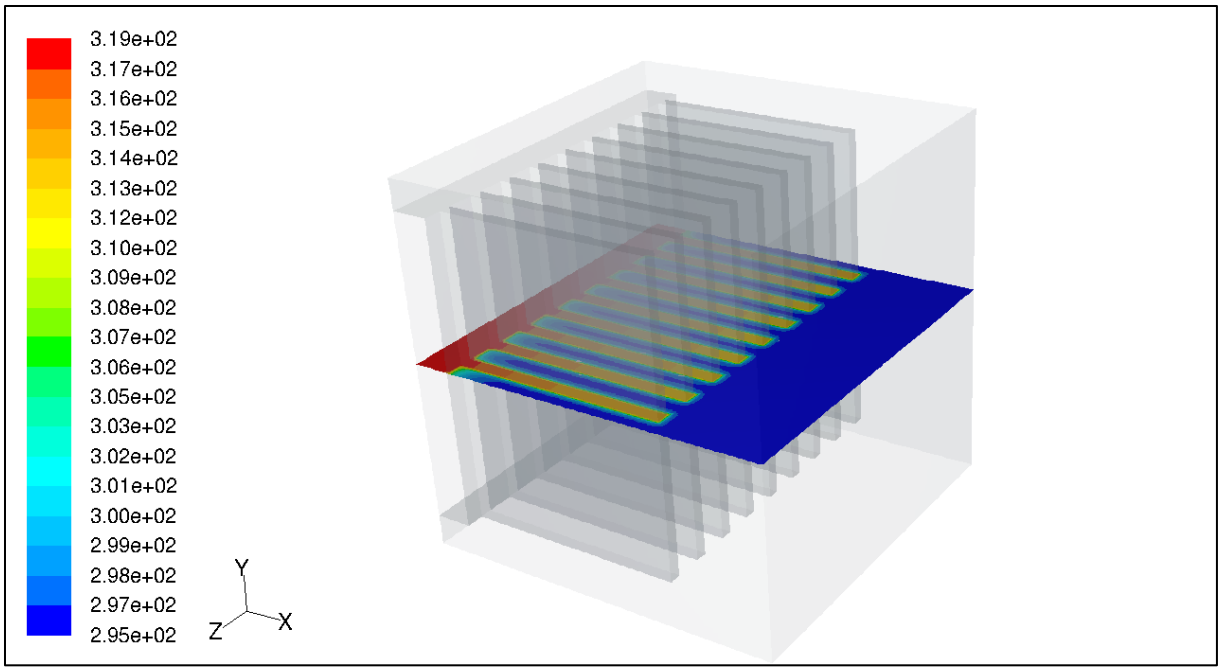

Figure 4.5 Temperature distribution with k-epsilon turbulence model using standard wall function (SWF)

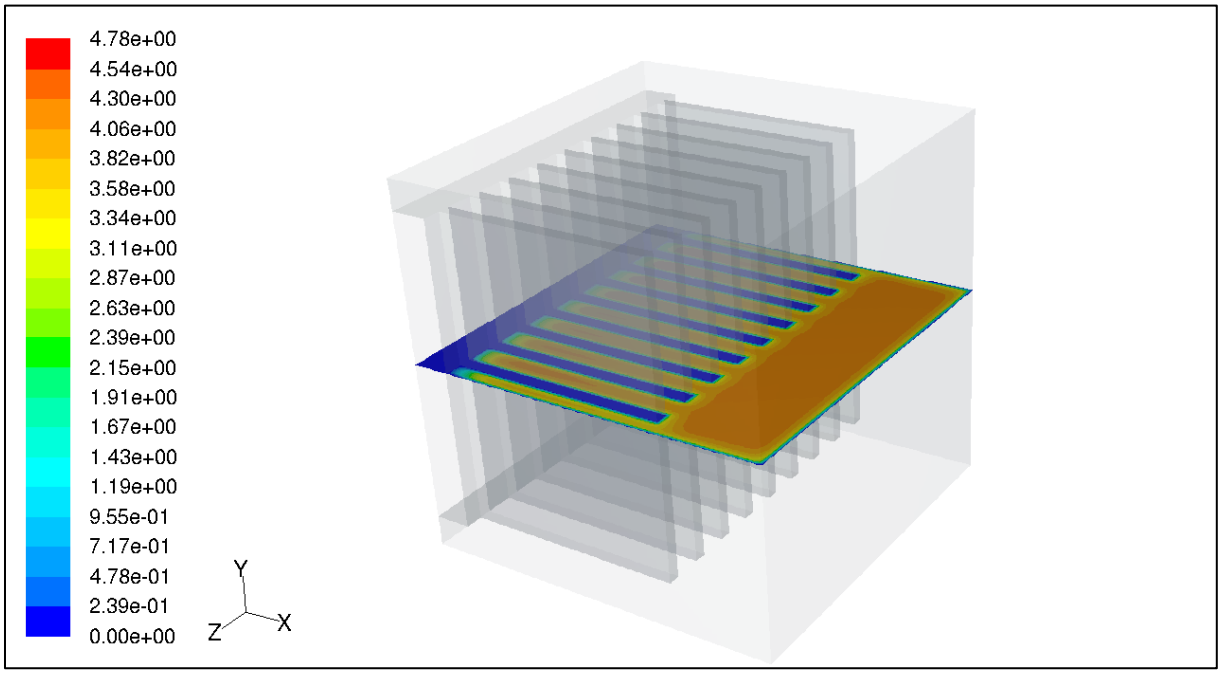

Figure 4.6 Velocity distribution with k-epsilon turbulence model using standard wall function (SWF)

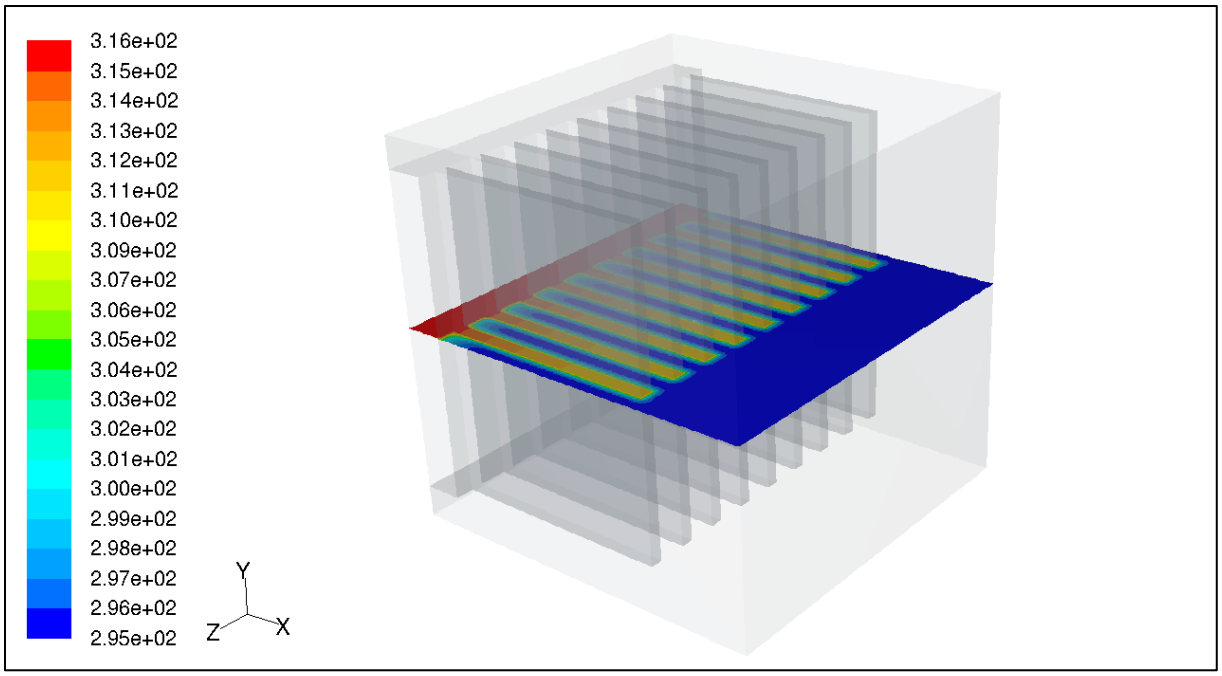

Figure 4.7 Temperature distribution with k-epsilon turbulence model using enhanced wall treatment (EWT)

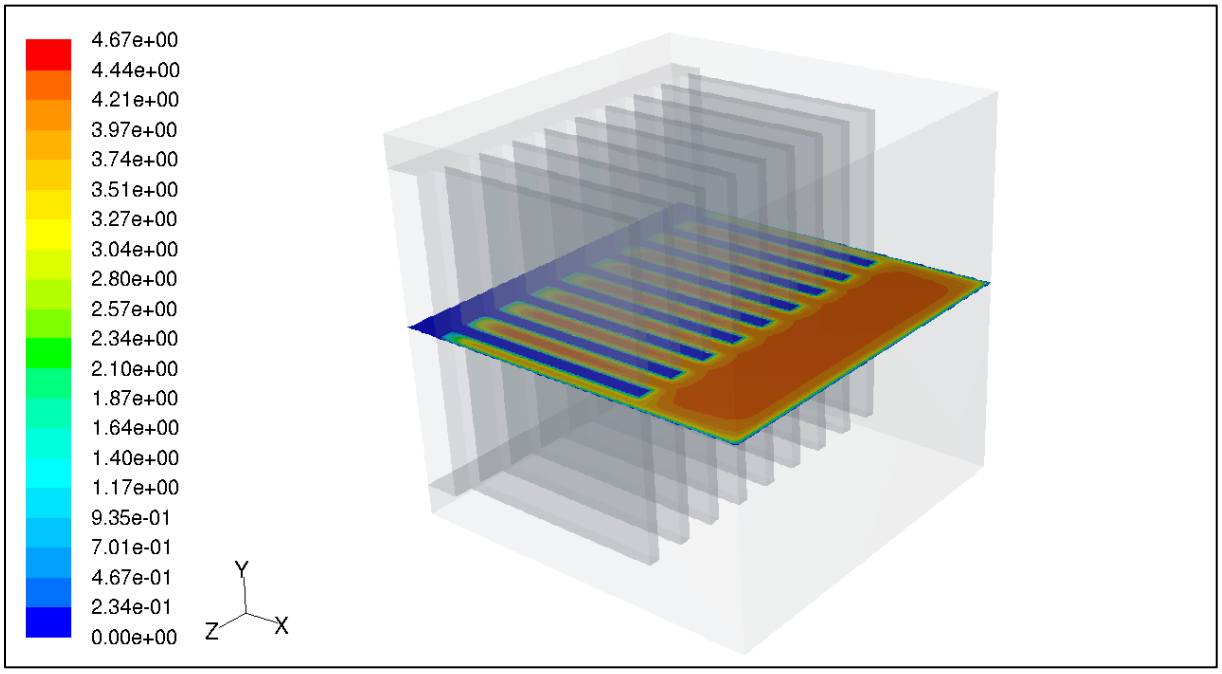

Figure 4.8 Velocity distribution with k-epsilon turbulence model using enhanced wall treatment (EWT)

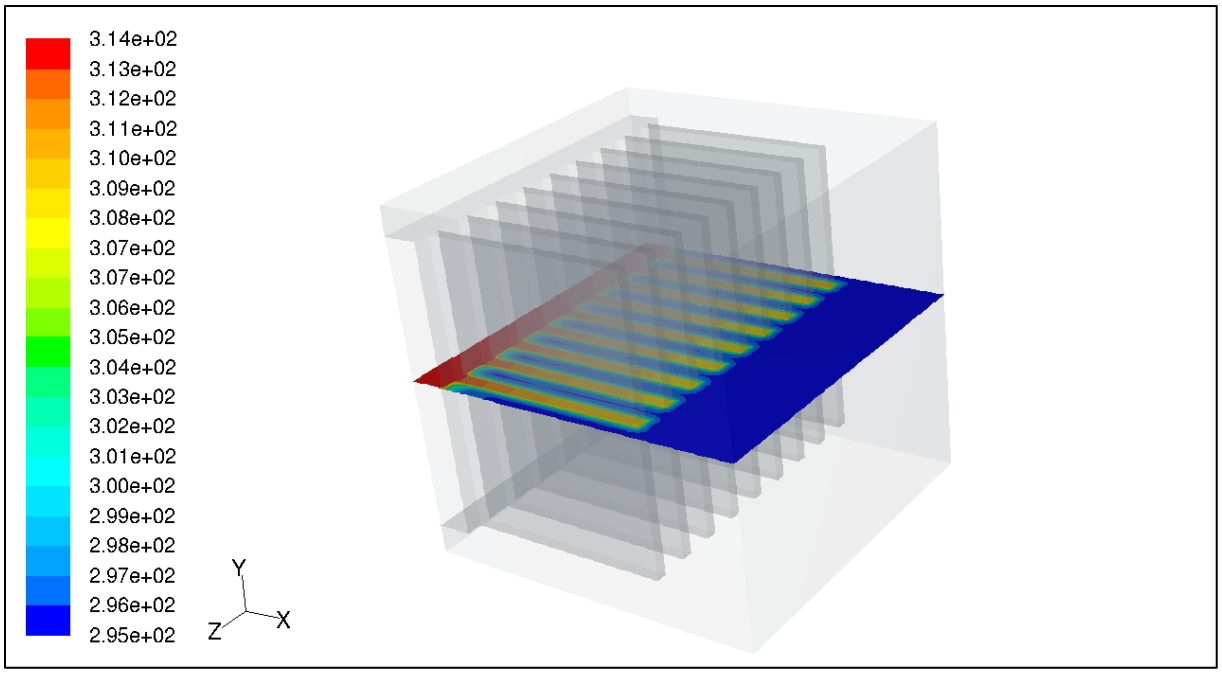

Figure 4.9 Temperature distribution with k-omega turbulence model

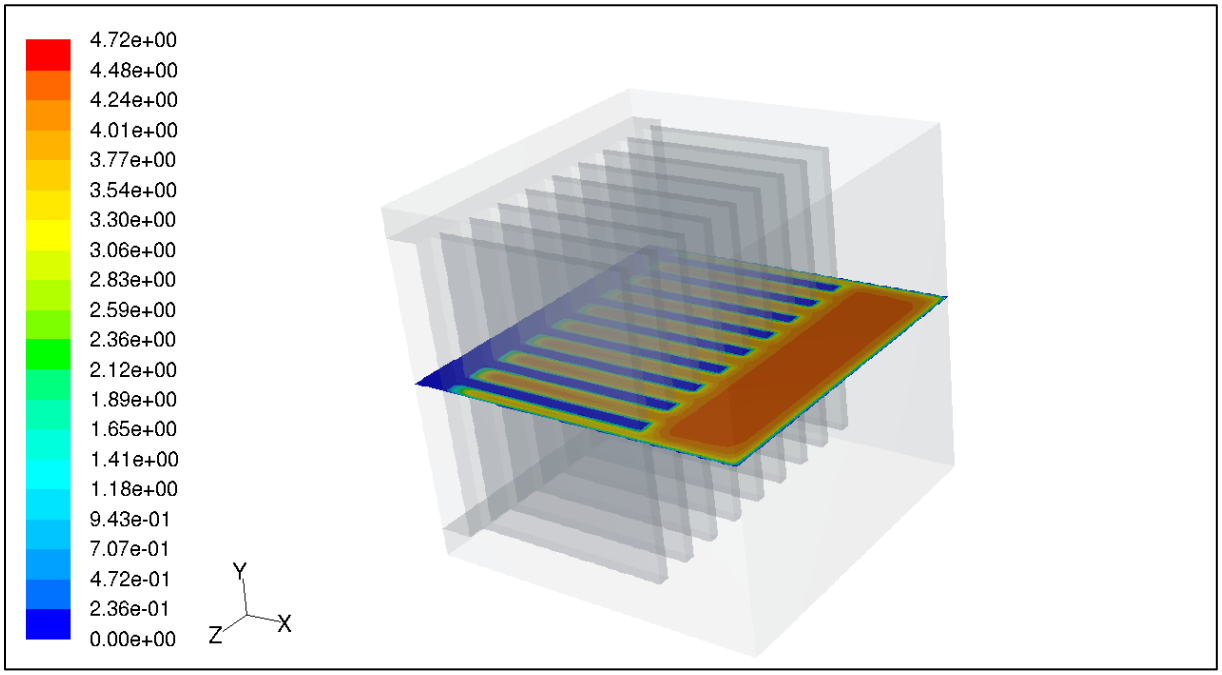

Figure 4.10 Velocity distribution with k-omega turbulence model

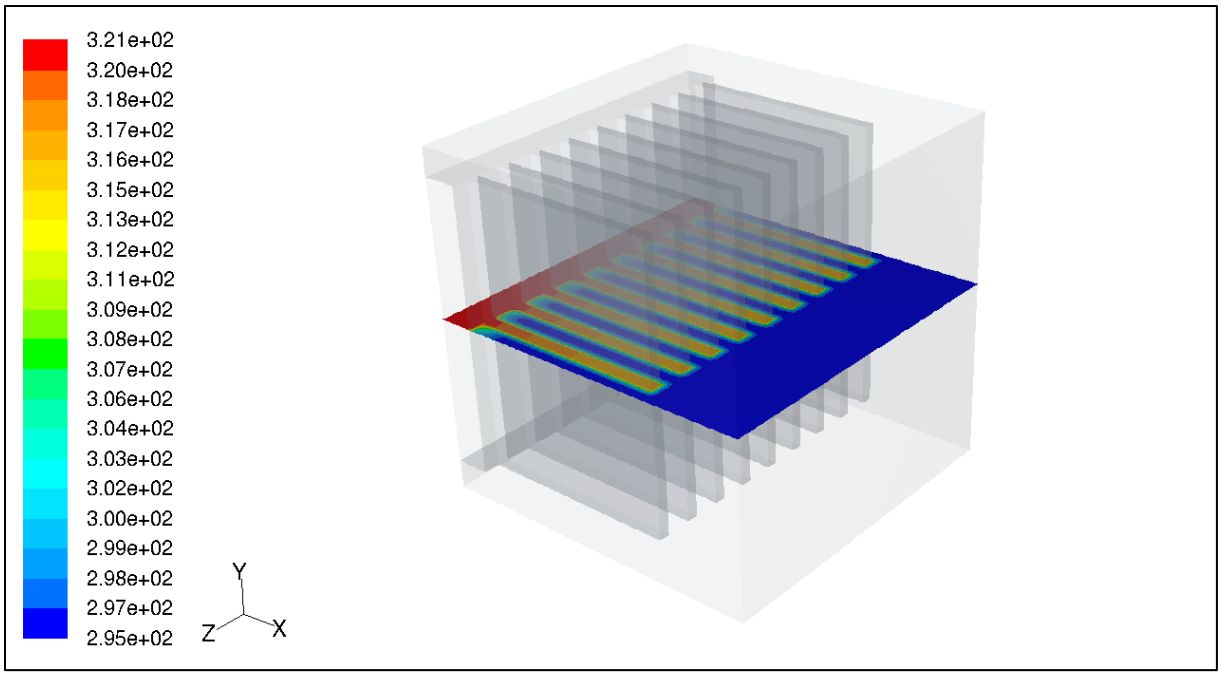

Figure 4.11 Temperature distribution with the Spalart-Allmaras turbulence model

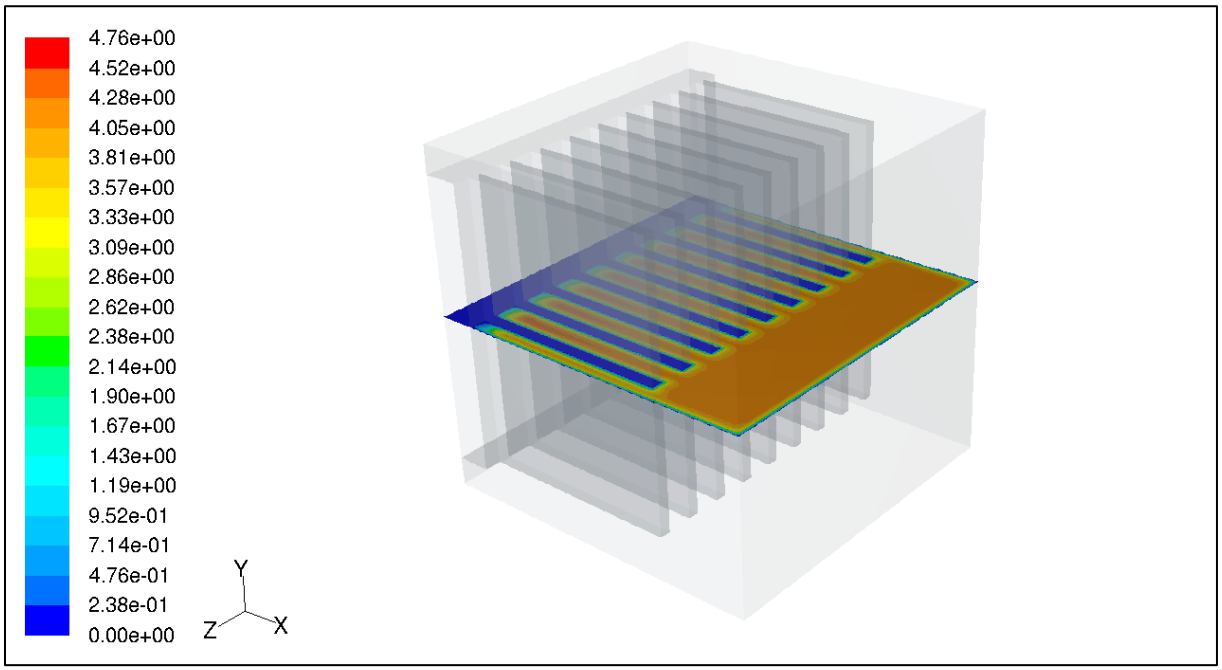

Figure 4.12 Velocity distribution with theSpalart-Allmaras turbulence model

4.1.3 Case 3

In case 3, pipe bundle heater element is used in experimental setup and in the modeling. In this part as similar to case 2 temperature and velocity profiles are displayed and the sectioning is perpendicular to the flow and in the middle of the fins. Temperature profiles for the specified turbulence models are displayed in Figures 4-13, 4-15, 4-17, 4-19. Velocity profiles are displayed in Figures 4-14, 4-16, 4-18, 4-20. Owing to the fins in the system, both conduction through the fins and convection heat transfer are solved as ‘coupled’.

Same discussion with the parallel plate fins can be stated for the fins which have pipe bundle design.

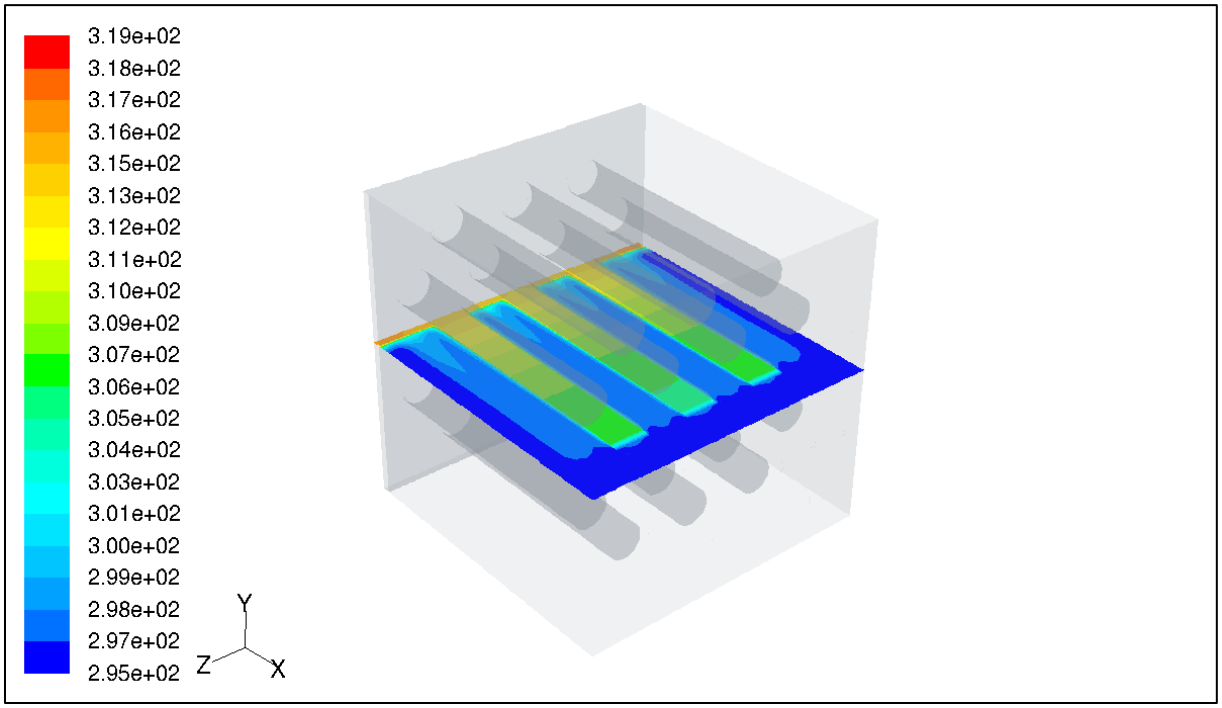

Figure 4.13 Temperature distribution with k-epsilon turbulence model using standard wall function (SWF)

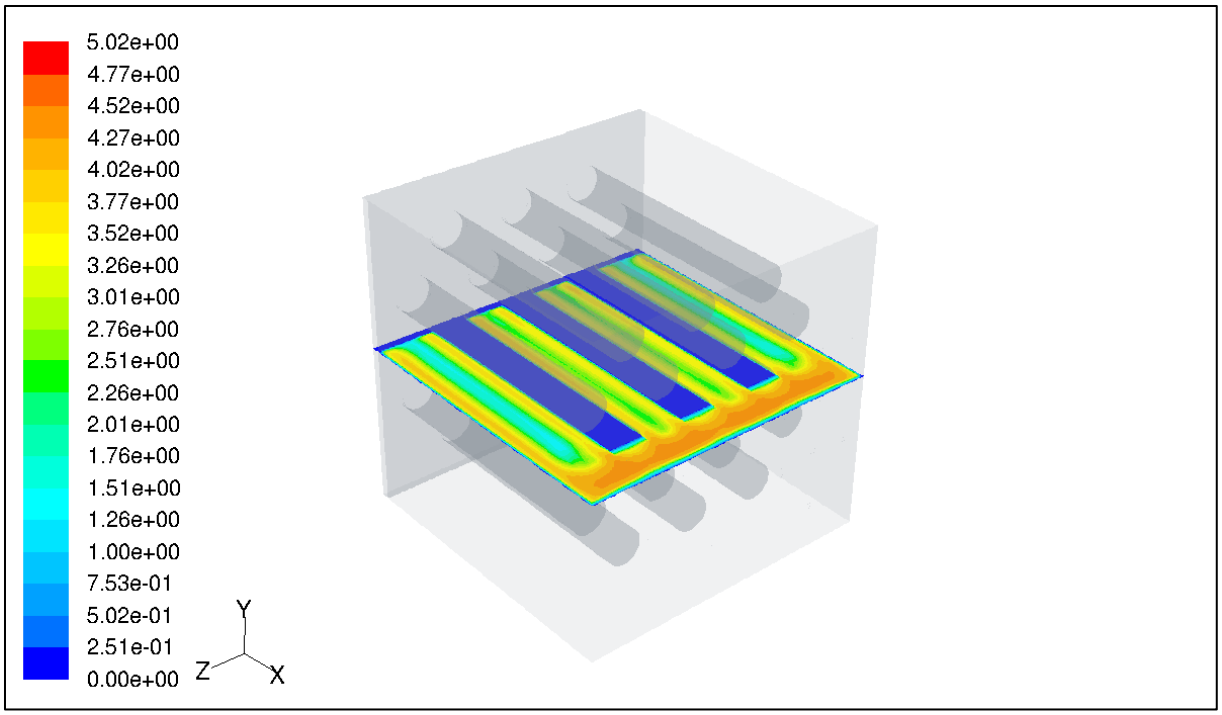

Figure 4.14 Velocity distribution with k-epsilon turbulence model using standard wall function (SWF)

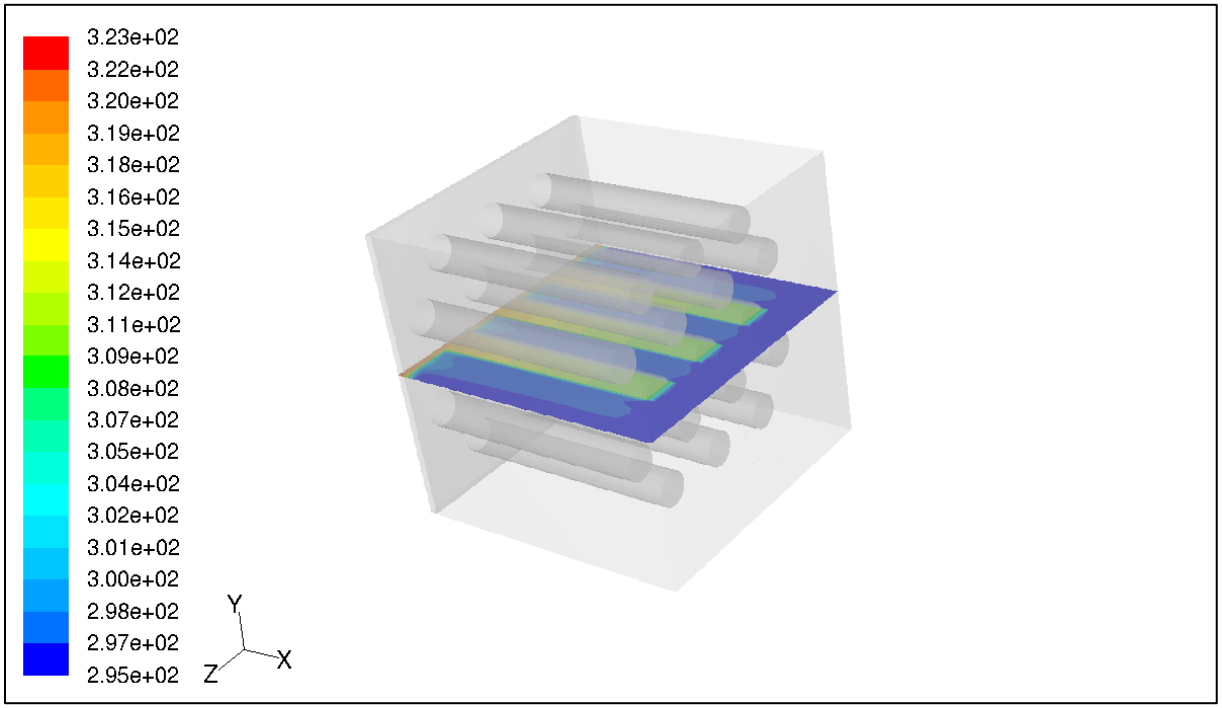

Figure 4.15 Temperature distribution with k-epsilon turbulence model using enhanced wall treatment (EWT)

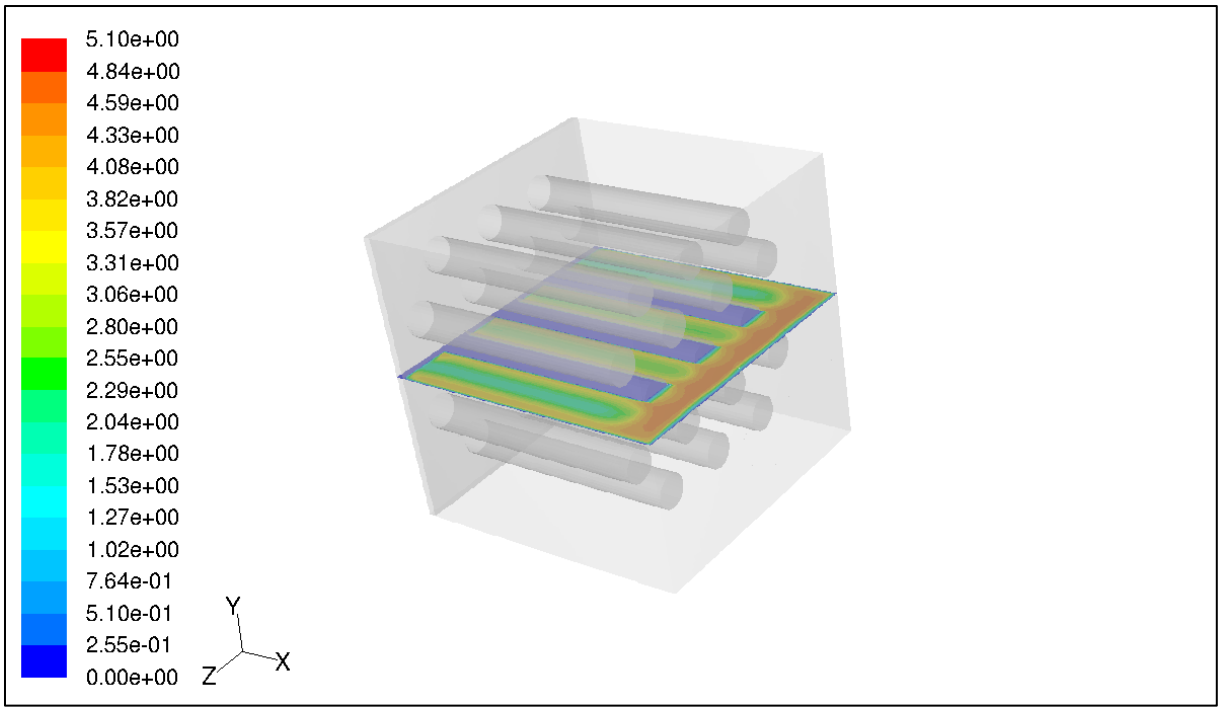

Figure 4.16 Velocity distribution with k-epsilon turbulence model using enhanced wall treatment (EWT)

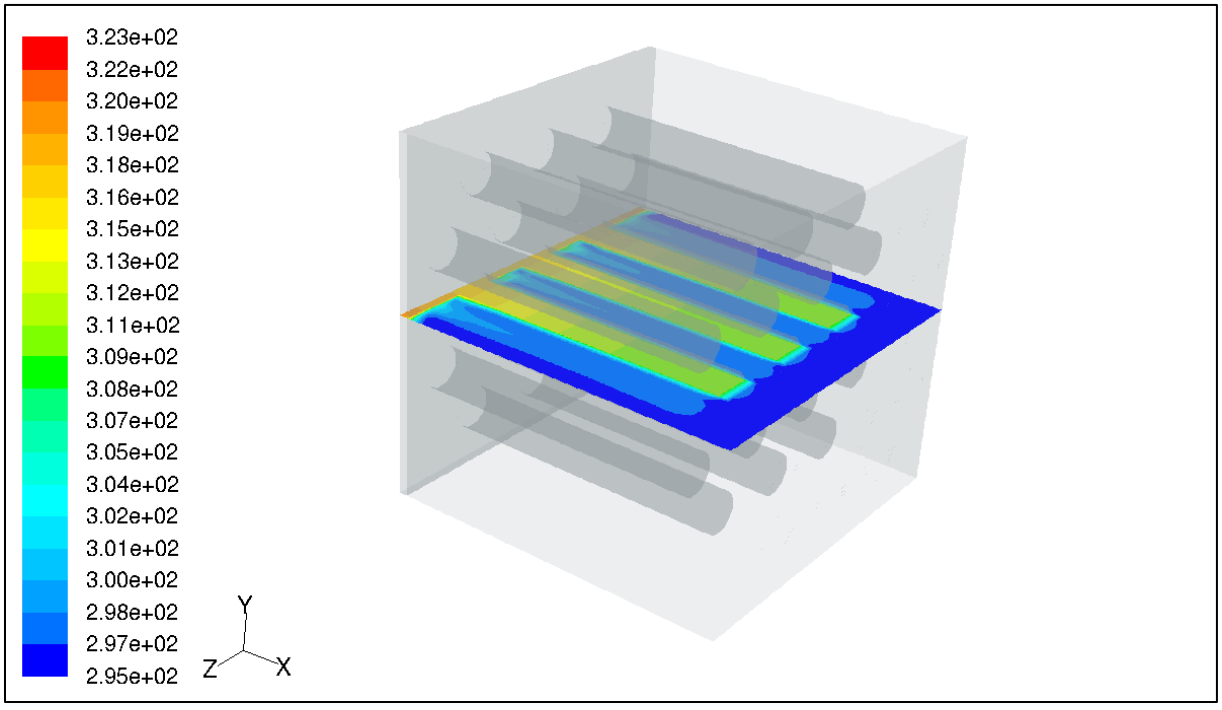

Figure 4.17 Temperature distribution with k-omega turbulence model

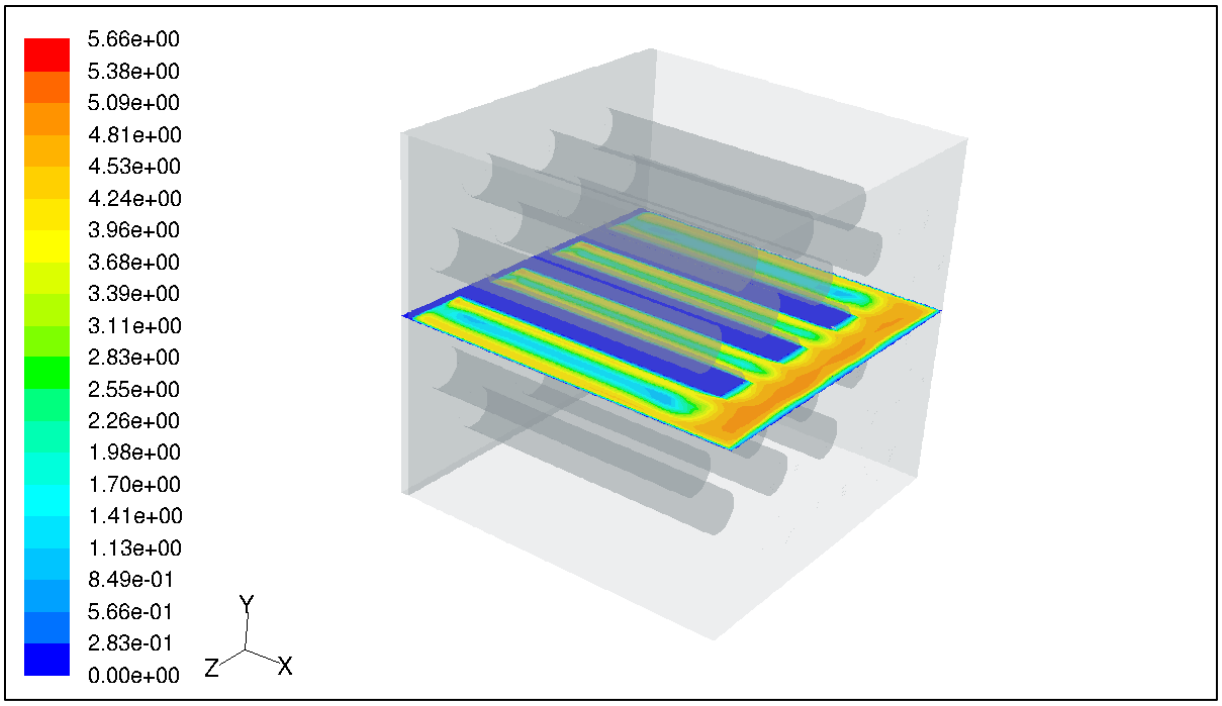

Figure 4.18 Velocity distribution with k-omega turbulence model

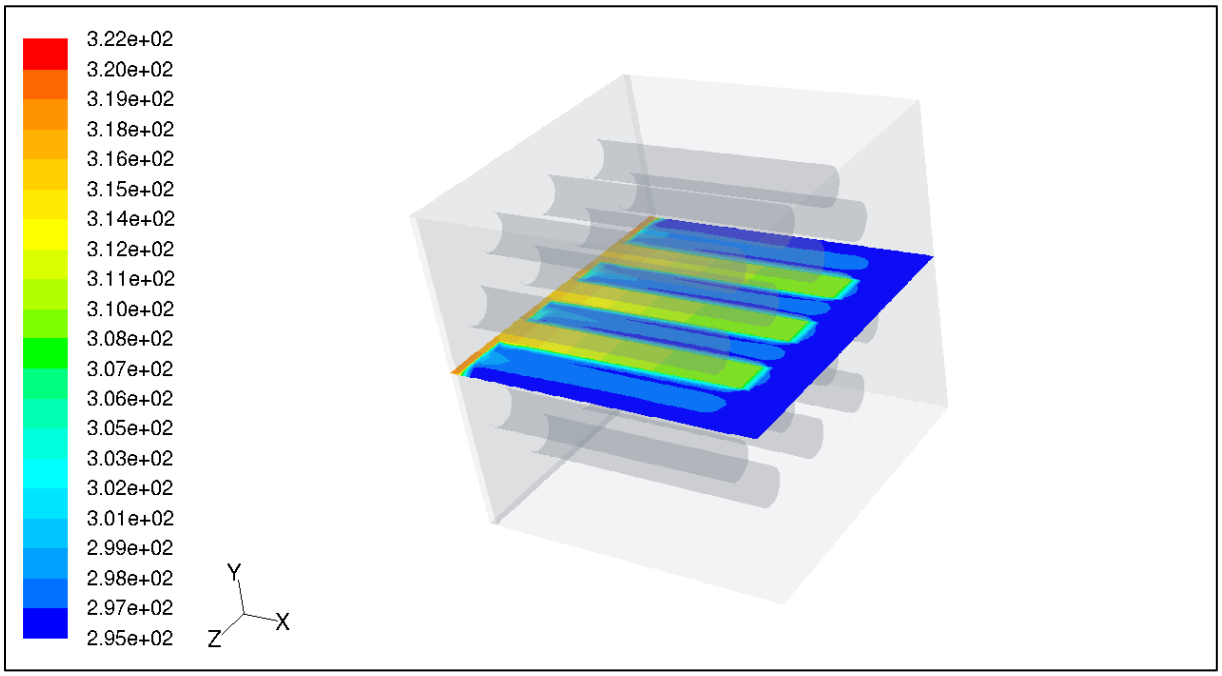

Figure 4.19 Temperature distribution with the Spalart-Allmaras turbulence model

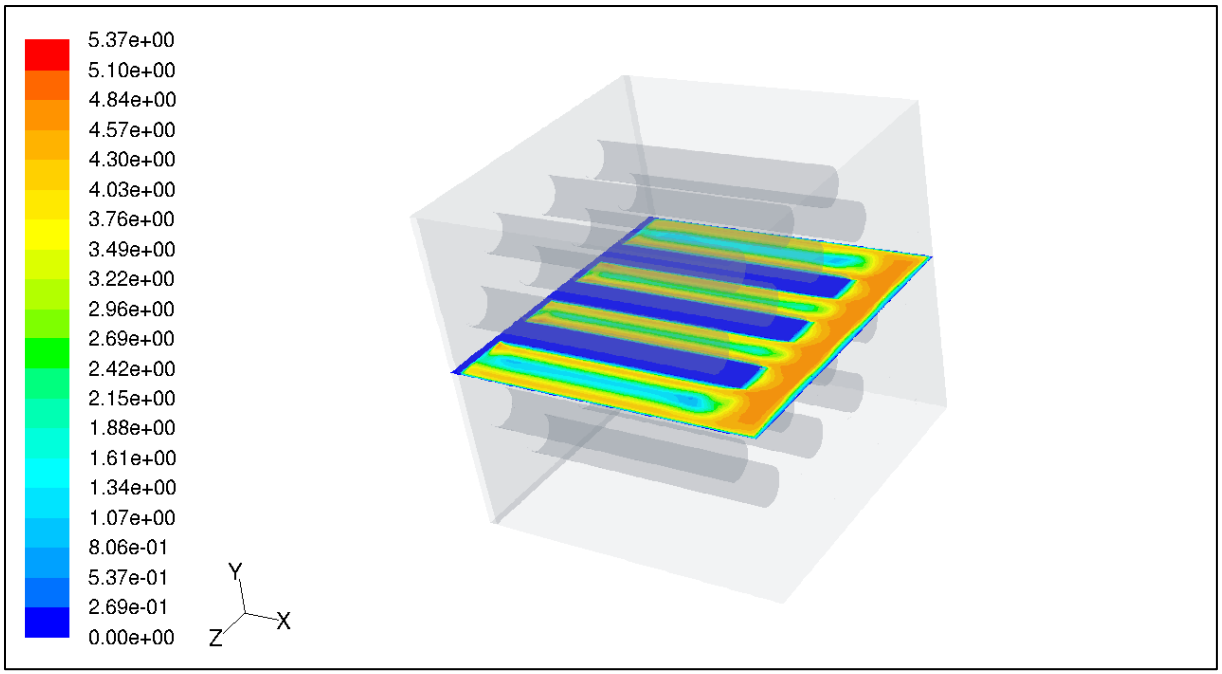

Figure 4.20 Velocity distribution with the Spalart-Allmaras turbulence model

4.2 Results of Analytical Calculations

In this part, the analytical calculations to calculate the Nusselt number and heat transfer coefficient are described for each case modeled. In order to select the proper experimental correlation or calculations, for each case the form of the flow (external or internal) is determined first and proper correlation is stated.

4.2.1 Case 1

The correlation for turbulent flow for this case is defined as the external flow despite of the enclosed geometry. For this case, the system was defined as checking the definition of an open system given by Incropera [6]. This definition sets values for temperature and velocity profiles which are valid for this case. Therefore the flow was assumed to be external flow. As the results of calculations performed with the internal flow correlations, it is shown that the fully developed region exceeded almost 10 times of the unit length and heat transfer coefficient turned out to be meaningless. Finally, Equation 1.5 is used to calculate theNusselt number and equation 2.3 and 2.5 are used to calculateReynolds number and heat transfer coefficient, respectively.

The data that is used for the calculations are tabled in 4.1 below.

Table 4.1Physical and geometrical data forCase 1

Velocity (u)-(m/s)	2.76
Inlet Temperature (T_{in})- (K)	295.35
Outlet Temperature (T_{out})- (K)	296.61
Length(L)- (m)	0.32
Density (ρ)-(kg/m^3)	1.09
Kinematic Viscosity(v)-(m^2/s)	$1.72*10^{-5}$
Specific Heat(c_p)-(J/kgK)	1007
Prandl Number (Pr)	0.707
Thermal Conductivity(k)-(w/m-K)	0.03

Reynolds number is calculated as defined in Equation 2.3,

$$Re = \frac{u\,L}{\nu} = \frac{2.76 * 0.32}{1.72e-5} = 51382.7$$

And Nusselt number is calculated from equation 1.5,

$$\overline{Nu_L} = 0.05544 Re_L^{4/5} Pr^{\frac{1}{3}} = 0.5544 * 51382.7^{4/5} 0.707^{\frac{1}{3}} = 289.96$$

Surface heat transfer coefficient is computed as determined in Equation 2.5,

$$h = \frac{kNu}{L} = \frac{0.03 * 289.6}{0.32} = 24.7\ w/m^2K$$

4.2.2 Case 2

Here the flow was assumed to be internal flow since the area between the fins isclose to each other. Internal flow is more convenient for the flow between fins. The flow is fully developed turbulent as the Reynolds number calculated by using Equation 1.11indicates [11]. The results show that Re_D is equal to 3054 and for this Reynolds number value the length for fully developed region is about 27 cm. So, fully developed region can be observed before the flow reach fins. Entrance length calculated shows that the internal flow assumption is valid for this case. The data for the calculations are listed in 4-2.

Table 4.2Physical and geometrical data for Case 2

Velocity (u)-(m/s)	2.54
Inlet Temperature (T_{in})- (K)	295.42
Outlet Temperature (T_{out})- (K)	298.08
Length(L)- (m)	0.015975
Density (ρ)-(kg/m^3)	1.09
Kinematic Viscosity(v)-(m^2/s)	1.72*10^{-5}
Specific Heat(c_p)-(J/kgK)	1007
Prandl Number (Pr)	0.707
Thermal Conductivity(k)-(w/m-K)	0.03

In the case of turbulent flow, typical length of entrance region is calculated from Equation 1.11;

$$I_e = 0.27\, m$$

The Nusselt number from Equation 1.13;

$$Nu_D = \frac{\left(\frac{f}{8}\right) Re_D Pr}{1.07 + 12.7\left(\frac{f}{8}\right)^{\frac{1}{2}}\left(Pr^{\frac{2}{3}} - 1\right)}$$

Hydraulic diameter is,

$$D_h = \frac{4A_c}{P} = \frac{4\,LS}{2\,(L+S)} = \frac{4 * 0.071 * 0.009}{2 * (0.071 + 0.009)} = 0.015975$$

Corresponding velocity between fins is,

$$V_{fin} = \frac{G}{N_{fin} b.H_f}$$

where G is the volumetric flow rate

N_{fin} is number of fins,

b is the gap between fins

H_f is the fin height.

$$V_{fin} = \frac{0.108 * 0.071 * 2.66}{9 * 0.009 * 0.071} = 3.55\, m/s$$

andthe Reynolds number is,

$$Re_{D_h} = \frac{uD_h}{\nu} = \frac{3.54 * 0.015975}{1.589e-5} = 3568.99$$

Hence flow is turbulent; friction factor is calculated from equation 1.12,

$$f = 0.316 * 3054^{-1/4} = 0.04088$$

The Nusselt number is;

$$Nu_D = \frac{\left(\frac{0.04088}{8}\right) * \ 3568.99 * 0.701}{1.07 + 12.7\ \left(\frac{0.04088}{8}\right)^{\frac{1}{2}} (0.701^{\frac{2}{3}} - 1)} = 14.65$$

Heat transfer coefficient is;

$$h = \frac{kNu}{L} = \frac{0.03 * 14.65}{0.015975} = 27.56\ w/m^2K$$

4.2.3 Case 3

For this case, heat transfer coefficient in a tube bank with staggered tube arrangement is calculated at film temperature. The data are in Table 4.3. For the flow across tube banks, Nusselt number is calculated by using Equation 1.6.

Table 4.3Physical and geometrical data for Case 3

Velocity (u)-(m/s)	2.18
Inlet Temperature (T_{in})- (K)	295.42
Outlet Temperature (T_{out})- (K)	298.44
Length(L)- (m)	0.015975
Density (ρ)-(kg/m^3)	1.09
Kinematic Viscosity(v)-(m^2/s)	$1.72*10^{-5}$
Specific Heat(c_p)-(J/kgK)	1007
Prandl Number (Pr)	0.707
Thermal Conductivity(k)-(w/m-K)	0.03
S_L	$1.5 * 10^{-2}$
S_T	$4 * 10^{-2}$
Diameter of bundles (m)	$1.4 * 10^{-2}$
C	0.4
m	0.6
C_2	0.92
Pr_s	0.700
Pr	0.701

By using Equation 1.7,

$$S_D = \left[0.015^2 + \frac{0.04^2}{2}\right]^{1/2} < \frac{0.04 + 0.014}{2}$$

$$S_D = 0.025 < 0.027$$

So V_{max}occurs at A_1 and $V_{max}$is calculated from equation 1.9 and $Re_{D,max}$ from 1.10.

$$V_{max} = \frac{0.04}{2(0.04 - 0.014)} 2.18 = 3.354\ m/s$$

$$Re_{D,max} = \frac{3.354 * 0.014}{20.92 * 10^{-5}} = 2244.4$$

$$C = 0.35 * \left(\frac{0.04}{0.015}\right)^{1/5} = 0.40$$

$$\frac{S_T}{S_L} = 2.67$$

Since rows of elements in the flow direction, N_L=5 From Table A.2; C_2=0.92

$$\overline{Nu_L} = 0.92 * 0.40 * 2244.4^{0.6} * 0.701^{0.36} \left(\frac{0.701}{0.700}\right)^{1/4}$$

$$\overline{Nu_L} = 33.26$$

Surface heat transfer coefficient;

$$h = \frac{k\ Nu}{D} = \frac{0.03 * 33.20}{0.014} = 64.64\ w/m^2K$$

4.3 Conclusion

As the results of analytical calculations and CFD Analysis, it is possible to design a system having fins by using CFD method.In the modeling it‘s seen that the important aspect is boundary condition determination since the finned geometries, especially cylindrical type of fins are complex geometries. At the intersection points between heater element and fins, separation of flow is observed in pipe bundle type therefore boundary layerdefined in detail for the mesh generation. In addition, for all cases fine meshis required except for Case 1.

The results for CFD analysis and analytical results are compared and the results of comparison are listed in Table 4.4 for Case 1, in Table 4.5 for Case 2, in Table 4.6 for Case 3. As tables show comparisons are made for the Nusselt number and surface heat transfer coefficient values. Relative error is calculated as the difference between the analytical and CFD results for surface heat flux. For Case1, analytical calculations are performed as described: the Nusselt number is calculated for the selection of a special case in which there is an unheated part, entrance region, and the heated part where the flat plate type heater element is placed. Defining the Nusselt number in FLUENT for Case 1 is observed after the correction of the reference values in “Report” subpart of the FLUENT menu and selection of the system with an area weighted average value. In Case 2 and Case 3, analytical calculations such as the Nusselt number and heat transfer coefficient are performed for a local area where the fins are placed. Defining the Nusselt number in FLUENT is observed not for the whole system but only for the fins for an area weighted average area value after the correction of the reference value as the same defined for Case 1.

Table 4.4 Comparison of heat transfer and the Nusselt number for different turbulence models and analytical calculations for Case 1

CASE 1	Analytical	K-epsilon-SWF	K-epsilon-EWT	K-omega	Spalart-Allmaras
Nusselt Number	289.96	322.52	326.18	360.64	271.71
Surface heat transfer coefficient ($w/m^2.K$)	24.70	27.41	27.73	30.65	23.10
Relative error for surface heat transfer coefficient%	-	9.78	12.27	24.00	6.4

Table 4.5 Comparison of heat transfer and the Nusselt number for different turbulence models and analytical calculations for Case 2

CASE 2	Analytical	K-epsilon-SWF	K-epsilon-EWT	K-omega	Spalart-Allmaras
Nusselt Number	13.08	15.10	18.80	20.77	14.32
Surface heat transfer coefficient ($w/m^2.K$)	27.56	30.04	35.30	39.00	26.90
Relative error for surface heat transfer coefficient %	-	8.99	28.1	41.5	9.53

As the tables present, analytical results of the Nusselt number and surface heat transfer coefficient are compared with theresults of FLUENT analysis performed with specified turbulence models. The results show that some models are in good agreement with analytical correlations. However some models is not convenient for modeling in FLUENT or more information about the unit should be known.

Table 4.6Comparison of heat transfer and the Nusselt number for different turbulence models and analytical calculations for Case 3

CASE 3	Analytical	K-epsilon-SWF	K-epsilon-EWT	K-omega	Spalart-Allmaras
Nusselt Number	33.26	36.09	28.48	27.71	25.27
Surface heat transfer coefficient ($w/m^2.K$)	64.64	77.61	61.03	59.38	54.15
Relative error for surface heat transfer coefficient %	-	20.06	5.58	8.13	16.22

Figures 4.1 through 4.4, as explained in Chapter 4.1, velocity profiles for different turbulent models are shown, as the comparisons between the results of the analytical calculations and the simulations show that the SpalartAllmaras is the best choice as a turbulence model for Case 1and 2; k-epsilon is the best choice for Case 3.

In Figures 4.21and 4.22 different turbulence models are compared for the temperature distribution along the fin in which it is placed at the center of the heated surface. Temperature distribution is obtained by creating a line in the middle of the fins. Turbulence models are the SpalartAllmaras, K-omega, and K-epsilon with enhanced wall treatment and standard wall function options. Finally these models are compared with the experimental values which are taken by temperature sensors along the fin.

All the models are in good agreement with each otherhowever they all estimated higher temperatures than experimental ones in Figure 4.21. This may be due to the error in sensors reading which is ±1, or due to the flow sensor which has a measurement accuracy ±0.15 m/s + 6% [22].As the Figure 4.21 is considered; with respect to thevalues of heat transfer coefficients of turbulence models in Table 4.6, the temperature distribution of experimental result along the fin is supposed to be at a higher value than the numerical results of different turbulent models. Since the experiment set up is not well insulated, the temperature distribution along the fins is lower than what is expected.

As it is determined that there is ± 1^{o}C error in temperature reading, this error produces about %33increase or decrease in surface heat flux since temperature difference between the inlet and outlet is almost 6 degrees and 1 ^{o}Cinfluence the boundary condition of heat flux.

In order to estimate the effect of error in heat flux calculations due to the error in temperature measurement or flow measurement, in the simulations, surface heat flux is increased % 10 and the results of the simulation is presented in Figure 4.23. As figure dictates that a measurement error leading to 10 % increase in surface heat flux causes 8^{o}C difference in surface temperature.

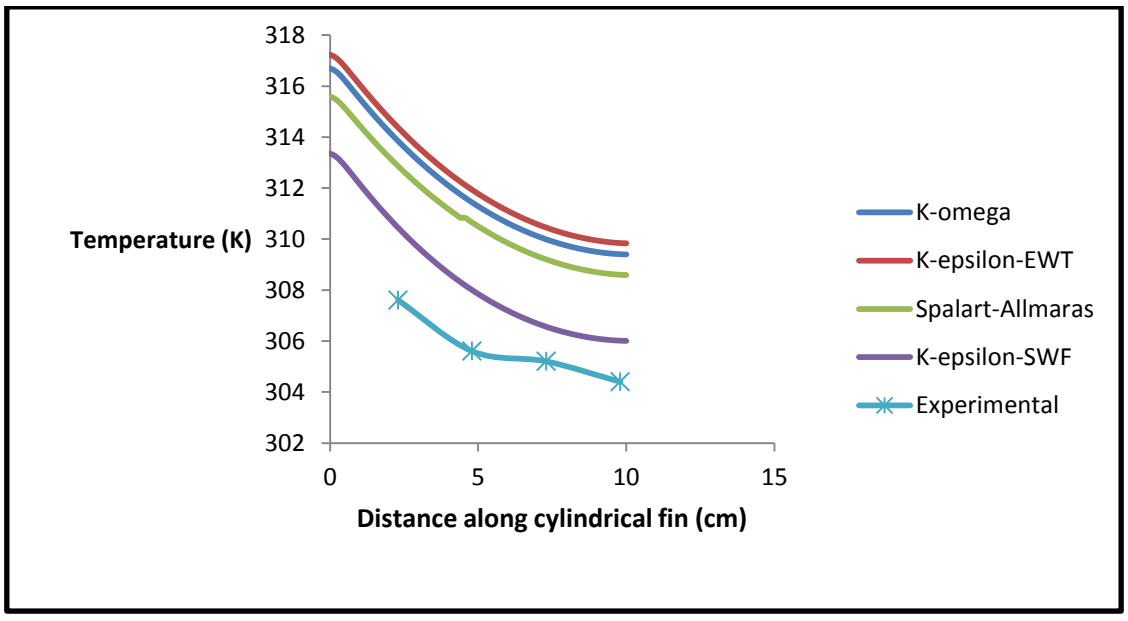

Figure 4.21Comparison of different turbulent models and experimental result for cylindrical fins

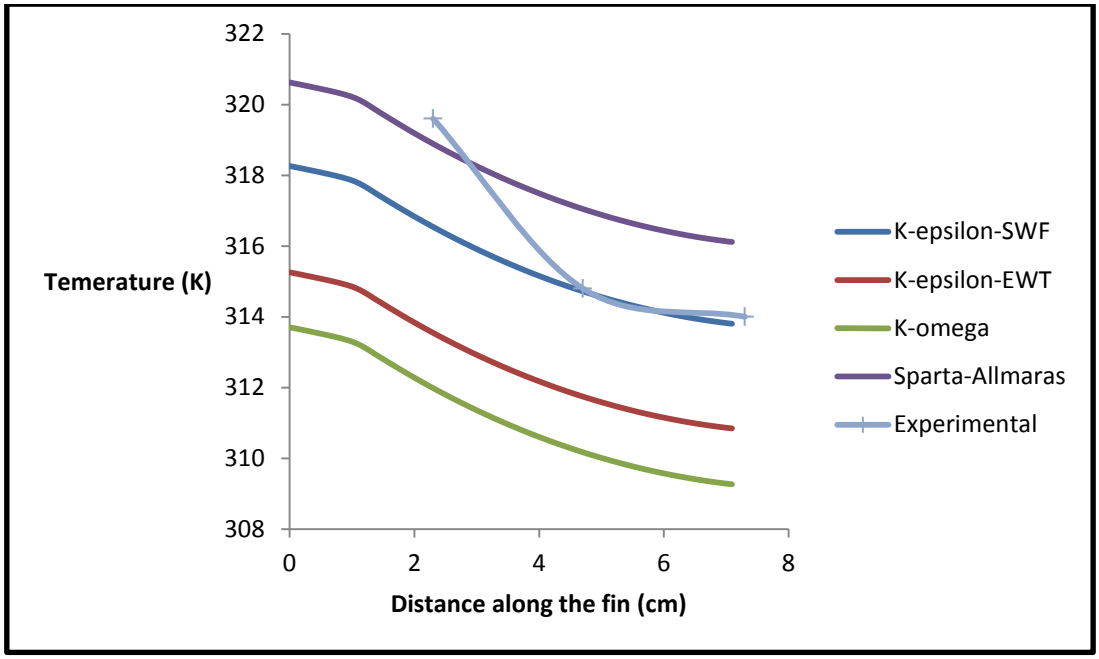

Figure 4.22Comparison of different turbulent models and experimental result for parallel fins

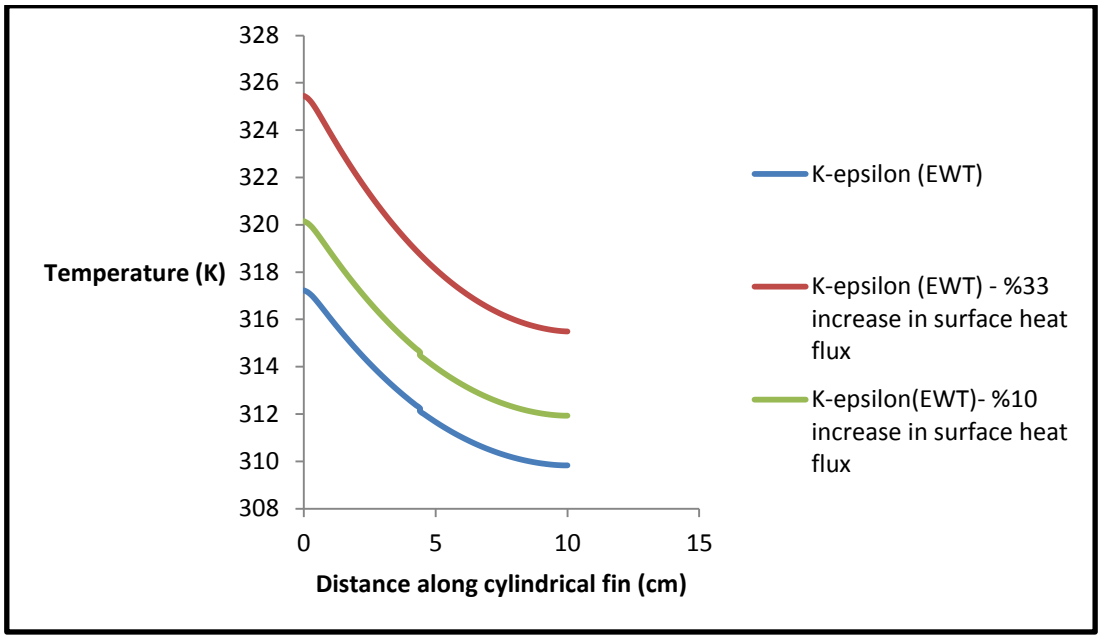

Figure 4.23Comparison of different surface heat fluxes for cylindrical fins

5 RECOMMENDATIONS FOR FUTURE WORK

Recommendations for future work are listed below,

1. Miscellaneous optimizations may be performed on fin models to achieve a more efficient system.
2. Instead of experimental data, custom parameters can be used for analytic calculations and FLUENT analysis which eventually minimize experimental error and produce more accurate results.
3. Instead of this experiment set, a new, well-adjusted and much more properly running experiment set may be preferred to achieve more accurate results.

REFERENCES

[1] Chung T.J.,Computational Fluid Dynamics, Cambridge University Press, 2002.

[2]Eymard, R., Gallouet,T., Herbin, R., Finite Volume Method, Handbook of Numerical Analysis, Ciarlet, P.G., Lions J.L. Eds, 2006.

[3]http://www.gunt.de

[4]Tu, J., Yeoh, G.H., Llu, C., A Practical Approach, Computational Fluid Dynamics, Butterworth-Heinemann Eds, USA, 2008.

[5] http://www.ansys.com/products

[6]Incropera, F.P., DeWitt, D.P., Intrdocution to Heat Transfer, 4th Ed., John Willey & SonsEds, USA, 2002

[7]FLUENT6.3 User's Guide

[8]Batchelor, G. K., An Introduction to Fluid Dynamics, Cambridge Univ. Press, Cambridge, England, 1967.

[9]Anderson, Jr., The Basics with Applications, Computational Fluid Dynamics, 1st Ed., McGraw-Hill Science/Engineering/Math Eds, 1995

[10] www.fluent.com

[11]Çengel, A. Y., Heat Transfer, 2nd Ed., McGraw-Hill Companies Eds., 2002.

[12] Soodphakdee, D., Behnia M., and Copeland, D.W., A Comparison of Fin Geometries for Heatsinks in Laminar Forced Convection: Part I - Round, Elliptical, and Plate Fins in Staggered and In-Line Configurations, The International Journal of Microcircuits and Electronic Packaging, vol. 24, Number 1, First Quarter, 2001, pp. 1063-1674.

[13] Khan, W.A., Modeling of Fluid Flow and Heat Transfer for Optimization of Pin-Fin Heat Sinks, PhD Thesis, University of Waterloo, Ontario, Canada, 2004.

[14]Guimarães, P.M., Da Silva, C.E.S., A parametric study of forced convection in an enclosure with stationary heated cylinders, International Communications in Heat and Mass Transfer, vol. 37, 2010, pp. 469–475.

[15]Al-Sarkhi A., Abu-Nada E., Characteristics of forced convection heat transfer in vertical internally finned tube, International Communications in Heat and Mass Transfer, vol. 32, 2005, pp. 557–564.

[16]Tahat M., Kodah Z.H., Jarrah B.A., Probert S.D., Heat transfers from pin-fin arrays experiencing forced convection, Applied Energy, vol. 67, 2000, pp. 419±442.

[17] Asharful Islam, Md., Mozumder A. K., Forced Convection Heat Transfer Performance Of An Internally Finned Tube, Journal of Mechanical Engineering, vol. 40, no.1, 2009.

[18]Nagarani N., Experımental Heat Transfer Analysis on Annular Circular and Elliptical Fins, International Journal of Engineering Science and Technology, vol. 2(7), 2010, pp. 2839-2845.

[19] Long, C., Sayma, N., Heat Transfer, Ventus Publishing Eds, 2009.

[20] http://www.cham.co.uk/phoenics/d_polis/d_lecs/general/turb.htm#1

[21] Tennekes, H., Lumley, J. L., A First Course in Turbulence, The MIT Press Eds., London, England, 1972.

[22] http://www.yuden-tech.com.cn/catalog/schmidt/ss20501-502.pdf

APPENDIX

Table A-0.1 Constants of equation for the tube bank in cross flow

Configuration	**$Re_{D,max}$**	**C**	**m**
Aligned	$10\text{-}10^2$	0.80	0.40
Staggered	$10\text{-}10^2$	0.90	0.40
Aligned	$10^2\text{-}10^3$	Approximate as a single (isolated) cylinder	
Staggered	$10^2\text{-}10^3$		
Aligned ($S_T/S_L>0.7$)[a]	$10^3\text{-}2 \times 10^5$	0.27	0.63
Staggered ($S_T/S_L<2$)	$10^3\text{-}2 \times 10^5$	$0.35(S_T/S_L)^{1/5}$	0.60
Staggered ($S_T/S_L>2$)	$10^3\text{-}2 \times 10^5$	0.40	0.60
Aligned	$2 \times 10^5\text{-}2 \times 10^6$	0.021	0.84
Staggered	$2 \times 10^5\text{-}2 \times 10^6$	0.022	0.84

[a] For ($S_T/S_L>0.7$), heat transfer is inefficient and aligned tubes should not be used.

Table A-0.2 Correction factor C2 for NL< 20 ($Re_{D,max} \geq 10^3$)

N_L	1	2	3	4	5	7	10	13	16
Aligned	0.70	0.80	0.86	0.90	0.92	0.95	0.97	0.98	0.99
Staggered	0.64	0.76	0.84	0.89	0.92	0.95	0.97	0.98	0.99

RESUME

Name Surname: Irmak ASLANTÜRK

Birth Place: İzmir, Turkey

Birth Date: June, 28 1984

Marital Status: Married

Language: Turkish (native), English, German

Education and Academic Positions:

- İzmir Atakent Anadolu High School, 1999-2002
- Undergraduate, Hacettepe University, Department of Nuclear Energy Engineering, 2002-2007
- Graduate, Hacettepe University, Department of Nuclear Energy Engineering, 2007-2010